PHYSICAL REVIEW B **81**, 245306 (2010)

Quantum coherence at low temperatures in mesoscopic systems: Effect of disorder

Yasuhiro Niimi,[1,2,*] Yannick Baines,[1] Thibaut Capron,[1] Dominique Mailly,[3] Fang-Yuh Lo,[4,5] Andreas D. Wieck,[4] Tristan Meunier,[1] Laurent Saminadayar,[1,6,†] and Christopher Bäuerle[1,†]

[1]*Institut Néel, CNRS and Université Joseph Fourier, BP 166, 38042 Grenoble, France*

[2]*Department of Physics, Tohoku University, 6-3 Aramaki-aza Aoba, Aoba-ku, Sendai, Miyagi 980-8578, Japan*

[3]*Laboratoire de Photonique et Nanostructures, route de Nozay, 91460 Marcoussis, France*

[4]*Lehrstuhl für Angewandte Festkörperphysik, Ruhr-Universität, Universitätsstraße 150, 44780 Bochum, Germany*

[5]*Department of Physics, National Taiwan Normal University, 88, Sec. 4, Ting-Chou Rd., Taipei City 11677, Taiwan*

[6]*Institut Universitaire de France, 103 Boulevard Saint-Michel, 75005 Paris, France*

(Received 12 November 2009; revised manuscript received 18 March 2010; published 8 June 2010)

We study the disorder dependence of the phase coherence time of quasi-one-dimensional wires and two-dimensional (2D) Hall bars fabricated from a high mobility GaAs/AlGaAs heterostructure. Using an original ion implantation technique, we can tune the intrinsic disorder felt by the 2D electron gas and continuously vary the system from the semiballistic regime to the localized one. In the diffusive regime, the phase coherence time follows a power law as a function of diffusion coefficient as expected in the Fermi-liquid theory, without any sign of low-temperature saturation. Surprisingly, in the semiballistic regime, it becomes independent of the diffusion coefficient. In the strongly localized regime we find a diverging phase coherence time with decreasing temperature, however, with a smaller exponent compared to the weakly localized regime.

DOI: 10.1103/PhysRevB.81.245306 PACS number(s): 73.23.−b, 73.63.Nm, 03.65.Yz, 73.20.Fz

I. INTRODUCTION

Quantum coherence in mesoscopic systems is one of the major issues in modern condensed-matter physics as it is intimately linked to the field of quantum information. The interaction of solid-state qubits with environmental degrees of freedom strongly affects the fidelity of the qubit and leads to decoherence. Consequently, the decoherence process limits significantly the performance of such devices and it is often regarded as a nuisance. It is hence important to understand the limitation to the electronic coherence not only from the fundamental point of view but also for the realization of qubit devices.

According to the Fermi-liquid (FL) theory,[1] the phase coherence time τ_ϕ is limited by any inelastic scattering events, such as electron-electron (e-e) interactions, electron-phonon (e-ph) interactions, or spin-flip scattering of electrons from magnetic impurities. In all cases, τ_ϕ is expected to diverge as the temperature goes to zero. Contrary to this expectation, experimentally τ_ϕ seems to saturate at very low temperatures. Mohanty *et al.*[2] have observed systematic low-temperature saturations of τ_ϕ for Au wires. This experiment has triggered a controversial debate whether the low-temperature saturation of τ_ϕ is really *intrinsic* or *extrinsic*. Golubev and Zaikin[3,4] (GZ) have claimed that τ_ϕ intrinsically saturates at zero temperature due to electron-electron interactions in the ground state. On the other hand, this low-temperature saturation of τ_ϕ can also be explained by various extrinsic reasons such as the presence of dynamical two-level systems,[5,6] the presence of a small amount of magnetic impurities,[7–20] radio-frequency-assisted dephasing,[21] etc. However, none of those extrinsic mechanisms has been able to rule out the possibility that there might be an intrinsic saturation of τ_ϕ at low temperature. For example, an extremely small amount of magnetic impurities can always explain the observed saturation of τ_ϕ.[10–13] This fact shows that one cannot clearly discriminate the intrinsic and extrinsic mechanisms only from the temperature dependence of τ_ϕ and another parameter is needed to distinguish them.

In order to settle the important debate about the decoherence at zero temperature, we have chosen to study the disorder dependence, in other words, the diffusion coefficient D dependence of τ_ϕ as the two different scenarios (Fermi-liquid description or intrinsic saturation) predict different D dependencies on τ_ϕ. Some attempts to measure the D dependence of τ_ϕ have been performed in metallic systems[2,22] as well as in semiconductor ones.[23] However, any clear conclusion could not be drawn from those experiments since it is difficult to vary D in a controlled way over a wide range.

In this paper, we report on the electronic phase coherence time τ_ϕ measurements in quasi-one-dimensional (1D) wires and two-dimensional (2D) Hall bars fabricated from a high mobility 2D electron gas (2DEG). Using an original ion implantation technique, as detailed in the next section, we can vary the diffusion coefficient D over 3 orders of magnitude without changing any other parameter, such as electron density, band structure, etc. In our previous work on the low-temperature decoherence as a function of D,[24] we have presented mainly results for quasi-1D wires of a single width. Here we present an exhaustive report concerning the disorder dependence for quasi-1D wires as well as 2D Hall bars. The dimensionality defined in this paper is determined in terms of the phase coherence length $L_\phi=\sqrt{D\tau_\phi}$ as follows; when L_ϕ is larger than the width of wire w but smaller than the length of wire L, the system is "quasi-1D." On the other hand, when $L_\phi \ll w < L$, it is "2D." Depending on the range of the diffusion coefficient D, several different regimes can be attained for quasi-1D systems, i.e., ballistic, semiballistic, diffusive, and strongly localized regimes. In this work, we present decoherence measurements in the semiballistic, diffusive, and strongly localized regimes for the quasi-1D system as well as in the weakly and strongly localized regimes for the 2D system.

The paper is organized as follows; in the next section, experimental details are described. In Sec. III, we review

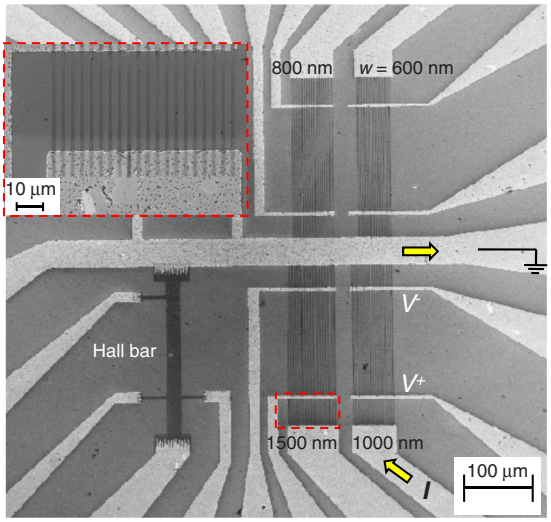

FIG. 1. (Color online) Scanning electron microscopy (SEM) image of the sample. The dark and white parts represent the mesas and electrodes, respectively. The voltage probes for the 1000 nm wide wires as well as the ground and current bias are added in the figure.

theories on the phase coherence time and weak localization (WL) in the diffusive (or weakly localized) regime, and then present experimental results in this regime. The results on the WL curves and the phase coherence time in the semiballistic regime are presented in Sec. IV. Section V is devoted to the discussion of the disorder dependence of the decoherence in quasi-1D wires. In Sec. VI, we discuss the *effective electron temperature* in our samples as it is a very important issue when discussing decoherence at zero temperature. Finally, in Sec. VII we present data for decoherence in the strongly localized regime.

II. SAMPLE FABRICATION AND EXPERIMENTAL SETUP

Samples have been fabricated from a GaAs/AlGaAs heterostructure grown in ultrahigh vacuum by molecular-beam epitaxy with electron density $n_e = 1.76 \times 10^{11}$ cm^{-2} and mobility $\mu_e = 1.26 \times 10^6$ cm^2/V s at a temperature of $T = 4.2$ K in the dark and before processing. All lithographic steps are performed using electron-beam lithography on polymethyl-methacrylate (PMMA) resist. Firstly, ohmic contacts have been patterned by evaporating an AuGeNi alloy onto the wafer. The wafer has been subsequently annealed at 450 °C for a few minutes in a hydrogen atmosphere. Secondly, the desired nanostructures (wires, Hall bars, etc.) have been etched into the MESA by argon ion milling over a depth of 5 nm using an aluminum mask. The mask has then been removed with a NaOH solution. Such a *shallow etching* results in highly specular reflection on the boundaries of the sample,[25] as discussed in Sec. IV B.

A scanning electron micrograph (SEM) of a typical sample used in this work is shown in Fig. 1. Each sample consists of four sets of wires of length $L = 150$ μm and of lithographic width $w = 600$, 800, 1000, and 1500 nm. In order to suppress universal conductance fluctuations (UCFs), each set consists of 20 wires connected in parallel. In addition, a

TABLE I. Formulas of some electronic parameters. The Drude conductivity $\sigma = \frac{1}{R_{xx}} \frac{L}{w}$ is obtained from the Hall bar.

Electron density n_e	$n_e = \frac{B}{eR_{xy}}$ or $n_e = \frac{eB\nu}{h}$ [a]
Fermi velocity v_F	$v_F = \frac{\hbar k_F}{m^*} = \frac{\hbar\sqrt{2\pi n_e}}{m^*}$
Elastic scattering time τ_e	$\tau_e = \frac{m^*\sigma}{e^2 n_e}$
Elastic mean-free path l_e	$l_e = v_F\tau_e = \frac{h\sigma}{e^2\sqrt{2\pi n_e}}$
Diffusion coefficient D	$D = \frac{1}{2} v_F l_e = \frac{\pi\hbar^2\sigma}{e^2 m^*}$
Electron mobility μ_e	$\mu_e = \frac{e\tau_e}{m^*} = \frac{\sigma}{n_e e}$
$k_F l_e$	$k_F l_e = \frac{h}{e^2}\sigma$

[a] ν is the filling factor.

Hall bar allows to measure the electronic parameters of the 2DEG: n_e, μ_e, elastic mean-free path l_e, elastic scattering time τ_e, etc. The diffusion coefficient is obtained via the relation $D = 1/2(v_F l_e)$, where v_F is the Fermi velocity. We summarize the formulas for the electronic parameters in Table I.

A large number of such samples is fabricated on the same wafer. In order to vary the disorder in our samples, we place a focused ion beam (FIB) microscope coupled to an interferometric stage on one sample using several alignment marks written on the wafer (Fig. 2). We then implant locally Ga^+ or Mn^+ ions with an energy of 100 keV into the sample. For such an energy, the implanted ions penetrate only about 50 nm into the GaAs heterostructure,[26] whereas the 2DEG lies 110 nm below the surface (inset of Fig. 2).[27] For the doses used here, the ions create crystal defects in the AlGaAs

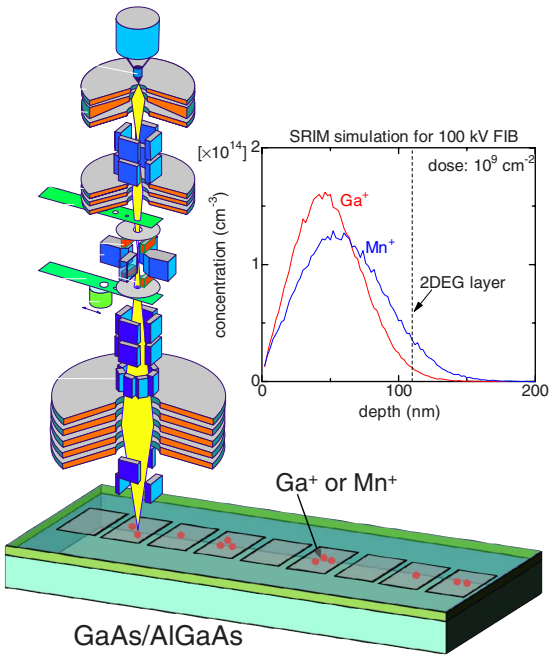

FIG. 2. (Color online) Schematic of a FIB microscope placed on the GaAs wafer. The inset shows an SRIM simulation (see Ref. 26) of the implanted ion concentration as a function of depth at a dose of 10^9 cm^{-2} and at an energy of 100 keV. The ions are predominantly implanted 50 nm above the 2DEG.

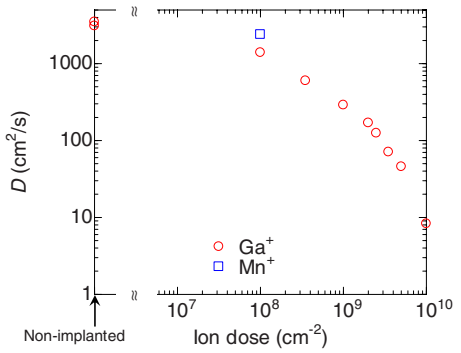

FIG. 3. (Color online) Diffusion coefficient as a function of ion dose for Ga^+ and Mn^+.

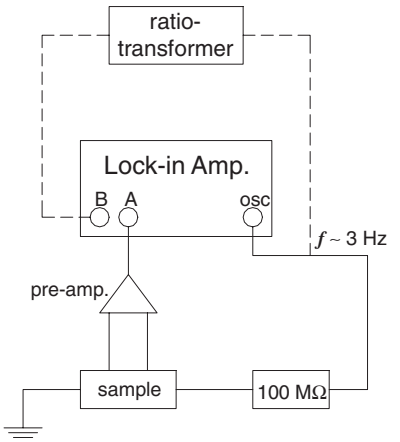

FIG. 4. Schematic of our electric circuit. A ratio transformer is used to subtract the background resistance and to extract the small WL signal above 1 K.

doped layer and modify the electrostatic disorder potential felt by the electrons. With this original setup we are thus able to change the intrinsic disorder of the samples on the same wafer by simply changing the implantation dose. For such low doses, the implanted ions affect only the elastic scattering time and the mobility of the itinerant electrons in the 2DEG,[28] but do not affect the band structure and the effective mass of GaAs.[29,30]

By varying the implantation dose for different samples from 10^8 to 10^{10} cm^{-2}, we are able to vary the diffusion coefficient from 3500 cm^2/s (unimplanted sample) to 8 cm^2/s. The diffusion coefficient variation as a function of implantation dose is shown in Fig. 3. Above an implantation dose of 10^9 cm^{-2}, we observe an important variation in the diffusion coefficient. The electronic parameters of all our samples are listed in Table II. These parameters have been measured at $T=1$ K for $D \geq 1400$ cm^2/s and 10 K for $D \leq 600$ cm^2/s.[31]

All measurements have been performed at temperatures down to 10 mK using a dilution refrigerator. The resistance of the sample is measured in a current source mode with a standard ac lock-in technique. A voltage generated from a signal generator (typically at a frequency of 3 Hz) is fed into the sample via a very stable resistance, typically on the order of 10–100 MΩ. The voltage across the quantum wire or the Hall bar is then measured between two voltage probes (see Fig. 1) and amplified by a homemade preamplifier situated at room temperature. This voltage amplifier has an extremely low noise voltage of about 0.5 $nV/\sqrt{Hz}$. Since the WL quantum correction above ~1 K is relatively small compared to classical background resistance ($<10^{-2}$), we have used a ratio transformer in a bridge configuration to compensate the large background signal. This allows us to increase the sensitivity of the WL measurement. A schematic of the measuring circuit is shown in Fig. 4. In order to avoid radio-frequency heating due to external noise, all measuring lines are extremely well filtered with commercially available highly dissipative coaxial cables, i.e., THERMOCOAX (Refs. 32 and 33) at low temperatures and with π filters situated at room temperature. The total attenuation at low temperature is more than −400 dB at 20 GHz. All experiments have been performed in thermal equilibrium which means that the applied voltage across the entire sample is kept such that the inequality $eV \leq k_B T$ is satisfied at all temperatures.

TABLE II. Characteristics of all our samples.

Ga^+ ion dose (cm^{-2})	D (cm^2/s)	l_e (nm)	μ_e ($cm^2/V\,s$)	n_e ($\times 10^{11}$ cm^{-2})	v_F ($\times 10^7$ cm/s)	$k_F l_e$	$T^* \equiv \hbar/(k_B \tau_e)$ (K)	$B^* \equiv m^*/(e\tau_e)$ (G)
0	3500	4000	6.2×10^5	1.56	1.7	400	0.33	160
0	3100	3600	5.5×10^5	1.56	1.7	350	0.36	180
1.0×10^8 [a]	2400	2800	4.4×10^5	1.49	1.7	270	0.46	230
1.0×10^8	1400	1700	2.6×10^5	1.50	1.7	160	0.78	390
6.0×10^8	600	660	9.7×10^4	1.72	1.8	69	2.1	1000
1.0×10^9	290	340	5.2×10^4	1.52	1.7	33	3.9	1900
2.0×10^9	170	200	3.1×10^4	1.48	1.7	19	6.6	3300
2.5×10^9	130	160	2.5×10^4	1.43	1.7	15	8.3	4100
3.5×10^9	71	95	1.7×10^4	1.16	1.5	8.1	12	6000
5.0×10^9	46	60	1.0×10^4	1.23	1.5	5.3	19	9500
1.0×10^{10}	8	12	2.4×10^3	0.94	1.3	0.95	81	40000

[a] Mn^+ ions are implanted.

III. DIFFUSIVE REGIME

A. Theory

1. Phase coherence time

In the weakly localized regime where $k_F l_e \gg 1$, the phase coherence time of electrons in a conductor is limited by inelastic scattering such as e-e interactions, e-ph interactions, the interaction with magnetic impurities (mag), or two-level systems (TLS), etc. In the presence of several decoherence mechanisms, the phase coherence time τ_ϕ can be expressed as

$$\frac{1}{\tau_\phi} = \frac{1}{\tau_{\text{e-e}}} + \frac{1}{\tau_{\text{e-ph}}} + \frac{1}{\tau_{\text{mag}}} + \frac{1}{\tau_{\text{TLS}}} + \cdots .$$

In the absence of extrinsic sources of decoherence, the phase coherence time at low temperatures is simply dominated by e-e interactions.[34] Thus, hereafter, we focus on the decoherence only due to e-e interactions.

In the FL theory without any disorder, the lifetime of quasiparticles follows a $(E-E_F)^{-2}$ power law, with E the energy and E_F the Fermi energy. In a real conductor, however, there is disorder. Altshuler, Aronov, and Khmelnitsky (AAK) took into account the disorder and the dimensionality of a conductor within the framework of the FL theory.[1] AAK showed that for a quasi-1D wire, the phase coherence time due to the e-e interactions can be expressed by

$$\frac{1}{\tau_{\text{e-e}}^{\text{1D}}} = aT^{2/3} \tag{1}$$

$$\equiv \alpha_{\text{AAK}} D^{-1/3} T^{2/3} \tag{2}$$

$$= \frac{1}{2}\left(\frac{k_B \pi}{w_{\text{eff}} m^*}\right)^{2/3} D^{-1/3} T^{2/3}, \tag{3}$$

where k_B is the Boltzmann constant and m^* is the effective mass of the electron. For a 2DEG made from a GaAs/AlGaAs heterostructure, $m^*=0.067m_e$, where m_e is the bare electron mass. w_{eff} is the effective width of the wire which is different from the lithographic width w given in the previous section because of lateral depletion effects inherent to the etching process. It should be noted that Eq. (3) has been demonstrated for the diffusive regime where the effective width w_{eff} is larger than the elastic mean-free path l_e such that the electron motion from one boundary to the other is diffusive.

In a similar way, the phase coherence time due to the e-e interactions for the 2D system is calculated as follows:

$$\frac{1}{\tau_{\text{e-e}}^{\text{2D}}} \simeq \frac{k_B T}{2m^* D} \ln\left(\frac{2m^* D}{\hbar}\right), \tag{4}$$

where $\hbar$ is the reduced Planck constant. Note that this expression is valid until the thermal length $L_T=\sqrt{\hbar D/k_B T}$ is larger than l_e. At higher temperatures such that $L_T \ll l_e$ [or $T \gg T^* \equiv \hbar/(k_B \tau_e)$], the dephasing process is not limited by disorder but simply by temperature as expected in the FL theory without disorder,[35]

$$\frac{1}{\tau_{\text{e-e}}^{\text{2D}}} \simeq \frac{m^* k_B^2 T^2}{4\hbar^3 n_e} \ln\left(\frac{2\pi\hbar^2 n_e}{k_B T m^*}\right). \tag{5}$$

In semiconductors, the crossover temperature $T=\hbar/(k_B\tau_e)$ is on order of 1 K.[36]

2. Weak localization correction

The measurements of the phase coherence time can be done in various ways such as measurements of WL,[9,13] Aharonov-Bohm conductance oscillations,[7,37,38] UCFs,[39,40] persistent currents,[41] etc. In this work, we have chosen to measure the phase coherence time of electrons via WL. Using this method, one can make the most reliable and quantitative discussion on the phase coherence time as shown in previous works.[2,8–14,24] The principle of this technique relies on constructive interference of closed electron trajectories which are "traveled" in opposite direction (time-reversed paths). This leads to an enhancement of the resistance. The magnetic field B destroys these constructive interferences, leading to a negative magnetoresistance $R(B)$ [or positive magnetoconductance $G(B)$] whose amplitude and width are directly related to the phase coherence time.

For a quasi-1D diffusive wire where $w_{\text{eff}} > l_e$, the WL correction is calculated as below[42]

$$\Delta G(B) \equiv G(B) - G(0) = -2N\frac{e^2}{h}\frac{L_\phi}{L}\left\{\frac{1}{\sqrt{1+\frac{L_\phi^2 w_{\text{eff}}^2}{3l_B^4}}} - 1\right\}, \tag{6}$$

where e^2/h is the quantum of conductance (e is the charge of the electron and h is the Planck constant), $l_B=\sqrt{\hbar/eB}$ is the magnetic length, and N is the number of wires in parallel ($N=20$ in the present case). The spin-orbit term has been neglected as spin-orbit coupling is very weak in GaAs/AlGaAs heterostructures. As discussed later on, we can obtain w_{eff} and $G(0)$ independently from the experimentally measured magnetoconductance and therefore the *only* fitting parameter is L_ϕ. By fitting the experimental magnetoconductance $G(B)$ with Eq. (6), we can obtain the phase coherence length L_ϕ at any temperature. The phase coherence time τ_ϕ is then extracted from the relation $L_\phi=\sqrt{D\tau_\phi}$. We note that Eq. (6) holds only when the magnetic field satisfies the inequality $l_B > w_{\text{eff}}$.[43] When $l_B < w_{\text{eff}}$, the lateral confinement becomes irrelevant for the WL and a crossover from 1D to 2D WL occurs.

If $L_\phi \ll w$, the 2D WL correction to the conductance is applied and given by

$$\Delta G(B) = \frac{e^2}{\pi h}\frac{w}{L}\left\{\Psi\left(\frac{1}{2}+\frac{l_B^2}{4L_\phi^2}\right) - \Psi\left(\frac{1}{2}+\frac{l_B^2}{2l_e^2}\right) + \ln\left(\frac{2L_\phi^2}{l_e^2}\right)\right\}, \tag{7}$$

where $\Psi(x)$ is the digamma function. The digamma function has the asymptotic approximation $\Psi(\frac{1}{2}+x) \simeq \ln x$ for large x. In the case of 2D WL, the characteristic field $B_c=\hbar/4eL_\phi^2$ which corresponds to one flux quantum through an area on the order of L_ϕ^2 is usually very small. For example,

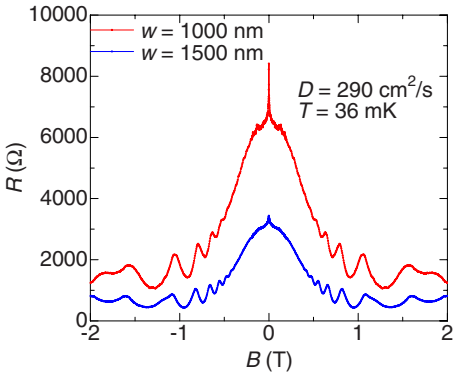

FIG. 5. (Color online) Magnetoresistance curves of 1000 and 1500 nm wide wires at $T=36$ mK and $D=290$ cm^2/s.

$B_c=1.6$ G for $L_\phi=1$ μm. The suppression of the WL effect is complete when $B>\hbar/2el_e^2$. These fields are always much weaker than classically strong fields $B^*\equiv m^*/(e\tau_e)$.

B. Experimental results

1. Quasi-1D wires

In order to determine the phase coherence length L_ϕ, we have performed standard magnetoresistance measurements as a function of temperature. A typical example for such a magnetoresistance curve is displayed in Fig. 5. Let us first concentrate on the field range up to a magnetic field of 2 T. A sharp peak which is due to WL is clearly seen at zero field. With increasing the magnetic field the WL peak disappears and another type of negative magnetoresistance is observed which is due to magnetic focusing. When going to even higher fields (>0.5 T) the well-known Shubnikov de Haas (SdH) oscillations appear.

Analyzing the WL peak allows to obtain the phase coherence length L_ϕ. In Fig. 6, we show magnetoconductance curves in units of e^2/h for $w=1000$ and 1500 nm wide wires at different temperatures. Note that the field scale is about three orders of magnitude smaller than that in Fig. 5. Since we are in a diffusive regime where l_e is smaller than w, the standard WL formula, Eq. (6), can be used. In Eq. (6), there are two parameters, i.e. L_ϕ, and $w_{\rm eff}$. The effective width $w_{\rm eff}$, however, is determined by fitting the magnetoconductance at a given temperature and diffusion coefficient. For lithographic widths $w=1000$ and 1500 nm, we obtain $w_{\rm eff}=630$ and 1130 nm, respectively. The effective width is then kept fixed for the entire fitting procedure and L_ϕ remains the only fitting parameter.

The observed WL curves are nicely fitted using Eq. (6) over the field ranges of ± 60 and ± 30 G for $w=1000$ nm and 1500 nm, respectively. At a higher field (above $\sim$100 G), however, the measured WL curves start to deviate from the theoretical fittings (insets of Fig. 6). For this reason, when we fit the magnetoconductance with the standard theory, we limit the field scale within $l_B>w_{\rm eff}$, i.e., $|B|<15$ and 5 G for $w_{\rm eff}=630$ nm and 1130 nm, respectively.

The extracted phase coherence length L_ϕ is plotted as a function of T at $D=290$ cm^2/s for $w=1000$ and 1500 nm wide wires in Fig. 7. At low temperatures, L_ϕ nicely follows

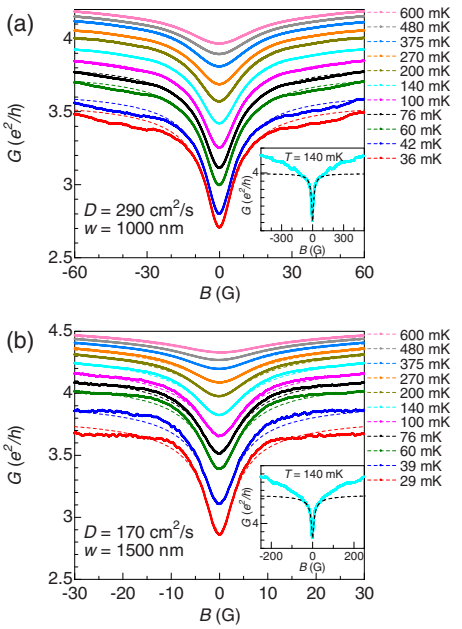

FIG. 6. (Color online) WL curves of (a) 1000 and (b) 1500 nm wide wires at $D=290$ cm^2/s and 170 cm^2/s, respectively. The conductance here is divided by e^2/h. The broken lines are the best fits of Eq. (6). The insets in (a) and (b) show the magnetoconductance at $T=140$ mK in larger field ranges.

a $T^{-1/3}$ law down to the lowest temperatures for both the wires. Note that the temperature below 40 mK has been corrected by measuring *in situ* the electron temperature of the quasi-1D wire based on e-e interaction corrections as detailed in Sec. VI. The absolute values of L_ϕ at low temperatures are different between the two wires, which is expected in the AAK theory in Eq. (3). Similar temperature dependence of L_ϕ has also been observed in GaAs/GaAlAs networks.[44]

Above $\approx$1 K, L_ϕ follows a T^{-1} law and its absolute value does not depend on the width of the wire. This is because L_ϕ is not limited by disorder any more but follows the FL theory without disorder as shown in Eq. (5).[23,35] When we fit the L_ϕ vs T curves, the following equation is used:

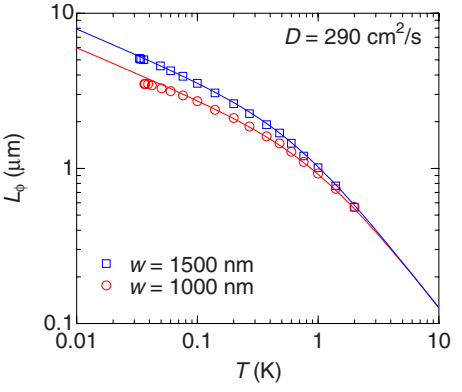

FIG. 7. (Color online) Phase coherence length of 1000 and 1500 nm wide wires as a function of T at $D=290$ cm^2/s. The solid lines are the best fits with Eq. (8).

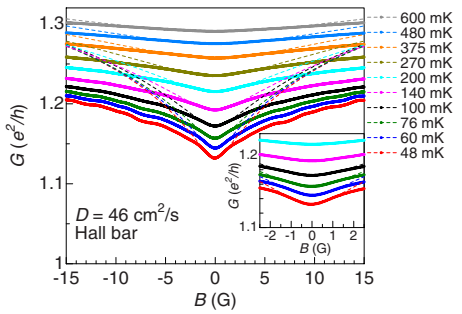

FIG. 8. (Color online) Magnetoconductance curves of a Hall bar at $D=46\ \mathrm{cm}^2/\mathrm{s}$ at different temperatures. The conductance is normalized by e^2/h. The broken lines are the best fits to Eq. (7). The fitted curves deviate from the experimental data at around B_c. The inset shows a closeup view of the low-field part of the magnetoconductance at low temperatures.

$$L_\phi = \sqrt{D\tau_\phi} = \sqrt{\frac{D}{a_{\mathrm{exp}}T^{2/3} + b_{\mathrm{exp}}T^2}}, \tag{8}$$

where a_{exp} and b_{exp} are the fitting parameters.[45]

2. Hall bars

In a similar manner to the quasi-1D case, the phase coherence length for Hall bars can also be extracted by fitting the WL curves with Eq. (7).[46,47] Figure 8 shows the WL curves of the Hall bar at $D=46\ \mathrm{cm}^2/\mathrm{s}$ at different temperatures and the best fits with Eq. (7). For these fittings we restrict the field scale to $B_c=\hbar/4eL_\phi^2$ for which 2D WL formula is applicable.[47,48] We recall that B_c is on the order of 1 G when $L_\phi=1\ \mu$m (see inset of Fig. 8). With increasing temperature, L_ϕ becomes smaller and the fitting region becomes larger as shown in Fig. 8. This clearly justifies the field limitation for the fittings.

The obtained L_ϕ of the Hall bar is plotted as a function of T in Fig. 9. At low temperatures, it follows a $T^{-1/2}$ law as expected in the AAK theory for 2D systems [see Eq. (4)]. On the other hand, L_ϕ has a T^{-1} dependence above ≈ 5 K where the thermal length L_T is smaller than l_e.[35] The whole L_ϕ vs T

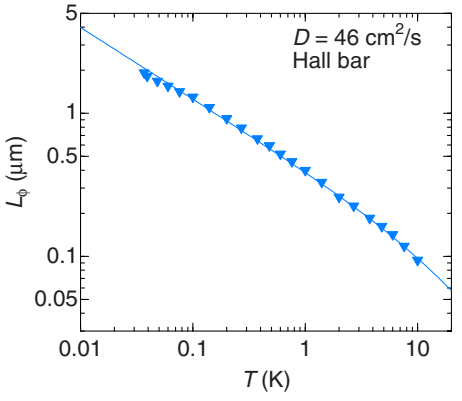

FIG. 9. (Color online) Phase coherence length of the Hall bar at $D=46\ \mathrm{cm}^2/\mathrm{s}$ as a function of T. The solid line is the best fit with Eq. (9).

curve of the Hall bar is fitted by combining Eqs. (4) and (5) as below

$$L_\phi = \sqrt{D\tau_\phi} = \sqrt{\frac{D}{a_{\mathrm{exp}}T + b_{\mathrm{exp}}T^2}}, \tag{9}$$

where a_{exp} and b_{exp} are the fitting parameters. The $\ln(T)$ term in Eq. (5) has been neglected here as we only measure the low-temperature regime.

IV. SEMIBALLISTIC REGIME

A. Theory

In this section, we review the WL theory for quasi-1D wires in the semiballistic regime where $w_{\mathrm{eff}} < l_e \ll L$. The WL in this regime has been studied theoretically by Beenakker and van Houten (BvH).[49] In such a clean limit, it is necessary to take into account specular reflections on the boundary of the wires and flux cancellation effects. Especially, the flux cancellation effect is of importance in the pure conductor regime, where the electrons move ballistically from one wall to the other. This effect leads to a wider WL curve compared to the diffusive case.

The WL correction in the semiballistic regime has been calculated by modifying the standard WL formula, Eq. (6),[49]

$$\Delta G(B) = -2N\frac{e^2}{h}\frac{L_\phi}{L}\left\{\left(\frac{1}{\sqrt{1+\frac{L_\phi^2}{D\tau_B}}}-1\right) - \left(\frac{1}{\sqrt{1+\frac{L_\phi^2}{D\tau_B}+\frac{2L_\phi^2}{l_e^2}}}-\frac{1}{\sqrt{1+\frac{2L_\phi^2}{l_e^2}}}\right)\right\}, \tag{10}$$

where τ_B is the magnetic scattering time. The first two terms are the same as Eq. (6) except $D\tau_B$ which is different from the diffusive case as discussed below. The last two terms come from a short-time cutoff. On short time scales $t < \tau_e$, the motion is ballistic rather than diffusive, and the return probability is expected to go to zero smoothly as one enters the ballistic regime. The short-time cutoff, on the other hand, should become irrelevant for $\tau_\phi \gg \tau_e$. Such a short-time cutoff has been inserted heuristically to compensate the ballistic motion in the WL correction.

In the semiballistic regime, τ_B has two limiting expressions depending on the ratio $w_{\mathrm{eff}}l_e/l_B^2$ as given below[49]

$$D\tau_B = \begin{cases} D\tau_B^{\mathrm{low}} = \dfrac{9.5}{2}\dfrac{l_B^4 l_e}{w_{\mathrm{eff}}^3} & \text{for } \sqrt{w_{\mathrm{eff}}l_e} \ll l_B \\ D\tau_B^{\mathrm{high}} = \dfrac{4.8}{2}\dfrac{l_B^2 l_e^2}{w_{\mathrm{eff}}^2} & \text{for } \sqrt{w_{\mathrm{eff}}l_e} \gg l_B \gg w_{\mathrm{eff}}. \end{cases}$$

The crossover from the "low" field and "high" field regions is well described by the interpolation formula

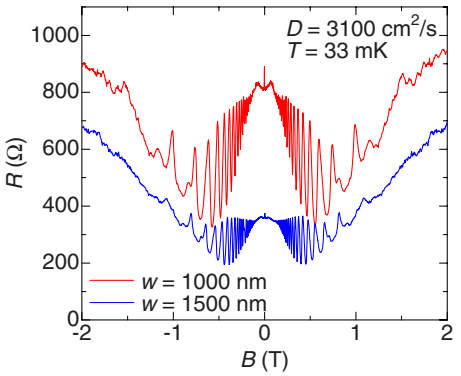

FIG. 10. (Color online) Magnetoresistance curves of 1000 and 1500 nm wide wires at $T=33$ mK and $D=3100$ cm^2/s.

$$D\tau_B = D\tau_B^{\text{low}} + D\tau_B^{\text{high}} = \frac{9.5}{2}\frac{l_B^4 l_e}{w_{\text{eff}}^3} + \frac{4.8}{2}\frac{l_B^2 l_e^2}{w_{\text{eff}}^2}. \quad (11)$$

This expression agrees well with numerical calculations[49] and is useful for comparison with experiments. The magnetic scattering time τ_B in Eq. (10) is then replaced by Eq. (11) within the field scale $l_B \gg w_{\text{eff}}$.

It should be stressed, on the other hand, that there is little knowledge on the decoherence time in the semiballistic regime, unlike the diffusive case discussed in Sec. III A.

B. Experimental results

As in the case of the diffusive regime, the phase coherence length L_ϕ in the semiballistic regime can be extracted by fitting experimental WL curves with Eq. (10). Before discussing the WL peak in a small field range, we show typical magnetoresistance curves of quasi-1D wires in the semiballistic regime in a field range of 2 T in Fig. 10. The overall structure of the magnetoresistance is similar to that in the diffusive regime (see Fig. 5); the WL peak near zero field and the SdH oscillation at high fields. In between these two structures, there is a small bump due to boundary roughness scattering[50,51] which does not exist in the diffusive regime. In the semiballistic regime where $l_e > w_{\text{eff}}$, the characteristics of the boundaries are of importance. Electrons are reflected specularly on the boundary with a given probability p. Otherwise, they are diffusively scattered into a random direction. In the case of shallow etching like in our case (see also Sec. II), the specular reflection probability p is more than 80% as reported in previous transport measurements on 2DEG samples.[25] The diffuse boundary scattering with a small probability $1-p$ (<20%) causes the observed small bump of the resistance in Fig. 10. In the presence of magnetic field, the electrons follow a curved trajectory and are scattered diffusively at each collision with the boundary. When the cyclotron radius R_c becomes comparable to the width of wire ($w_{\text{eff}}/R_c \approx 0.55$),[52] the resistance exhibits a maximum and then decreases again with increasing field because of the absence of backscattering. As is shown in Fig. 11(a), the maximum of the bump is located at 650 G, which corresponds to $B_{\max}=0.64\hbar k_F/ew_{\text{eff}}$ (i.e., $w_{\text{eff}}/R_c=0.64$). On the other hand, the amplitude of the bump is less than 5% compared to the background resistance. This result indicates that the probability of the diffusive boundary scattering is quite low,[50] which is consistent with the above statement (i.e., $1-p<20\%$). The observed bump structure vanishes with decreasing D or increasing disorder [Figs. 11(b) and 11(c)].

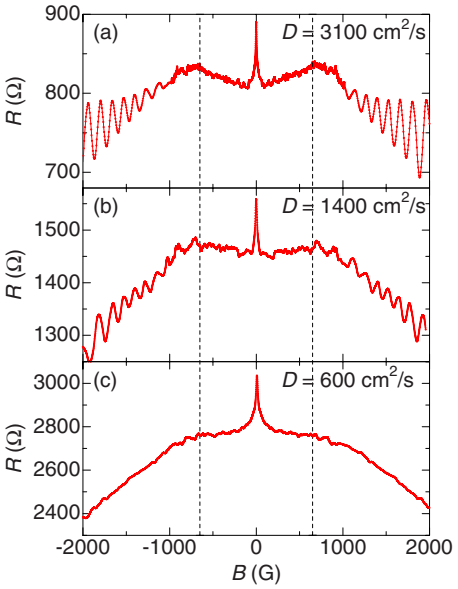

FIG. 11. (Color online) Magnetoresistance curves of 1000 nm wide wires at three different diffusion coefficients; (a) $D=3100$, (b) 1400, and (c) 600 cm^2/s. The broken line shows the maximum position of the small bump, i.e., $B_{\max}$.

Next, we focus on the WL peak on a smaller field scale. We show magnetoconductance curves in Fig. 12 for three different wire widths at different temperatures. As discussed in Sec. III B, the WL peak grows and becomes sharper with decreasing temperature for all the wires. The width of the WL peak, however, is almost the same as in the diffusive case (see Fig. 6). This is due to flux cancellation effects as mentioned above.

The phase coherence length L_ϕ in the semiballistic regime is obtained by fitting the WL curve with Eq. (10). Note that there are three parameters in Eq. (10), namely, L_ϕ, w_{eff}, and l_e. The effective width w_{eff} is, however, determined in the same way as in the diffusive case. For lithographic widths $w=1500$, 1000, and 600 nm, we obtain $w_{\text{eff}}=1130$ nm, 630 nm, and 230 nm, respectively. The elastic mean-free path l_e is also obtained from an independent measurement on the Hall bar having the same diffusion coefficient. Thus, there is again only one fitting parameter left, i.e., L_ϕ.

The broken lines in Fig. 12 show the best fits of Eq. (10). The WL curves of the three wires are nicely fitted by Eq. (10) at low fields while deviations from the theoretical fits occur at higher fields. As shown in Sec. IV A, the BvH expression is valid only within $l_B \gg w_{\text{eff}}$. Therefore, for fitting the magnetoconductance curves at any temperature we take into account only the low-field data and restrict the field range within $|B|<5$, 10, and 30 G for $w_{\text{eff}}=1130$ nm, 630 nm, and 230 nm, respectively.[53] Note that these fields are much larger than $B=\hbar/ew_{\text{eff}}l_e$ ($\sqrt{w_{\text{eff}}l_e} \gg l_B$). This means that we still have to take into account both the low- and high-field regions as pointed out in Eq. (11). The obtained L_ϕ at

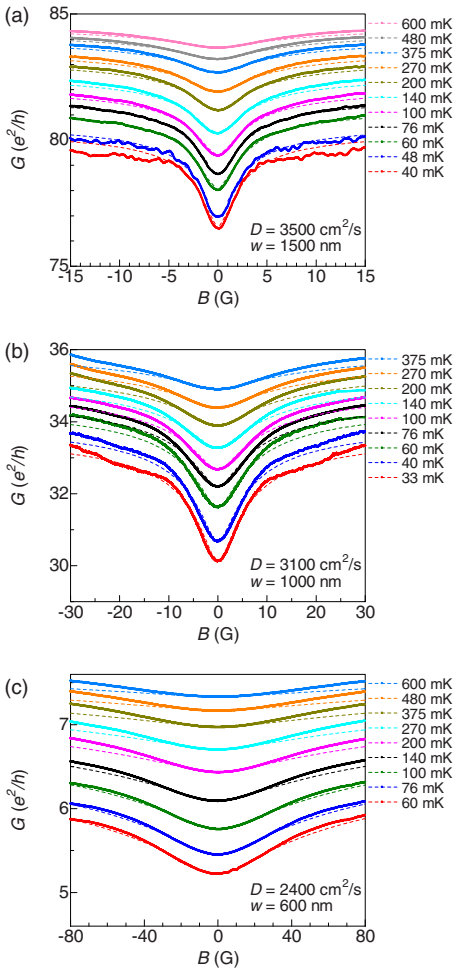

FIG. 12. (Color online) WL curves of (a) 1500, (b) 1000, and (c) 600 nm wide wires at D=3500 cm^2/s, 3100 cm^2/s, and 2400 cm^2/s, respectively. The conductance is normalized by e^2/h. The broken lines are the best fits to Eq. (10).

D=3500 cm^2/s is plotted as a function of T in Fig. 13. As in the diffusive regime, L_ϕ follows a $T^{-1/3}$ law at low temperatures and varies linearly with T above $\approx$1 K. Such a temperature dependence is indeed expected in the semiballistic regime.[54]

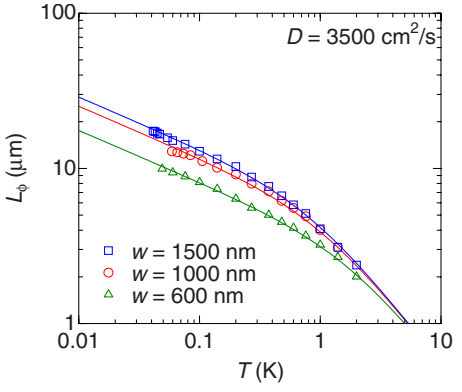

FIG. 13. (Color online) Phase coherence length of 1500, 1000, and 600 nm wide wires as a function of T at D=3500 cm^2/s. The solid lines are the best fits with Eq. (8).

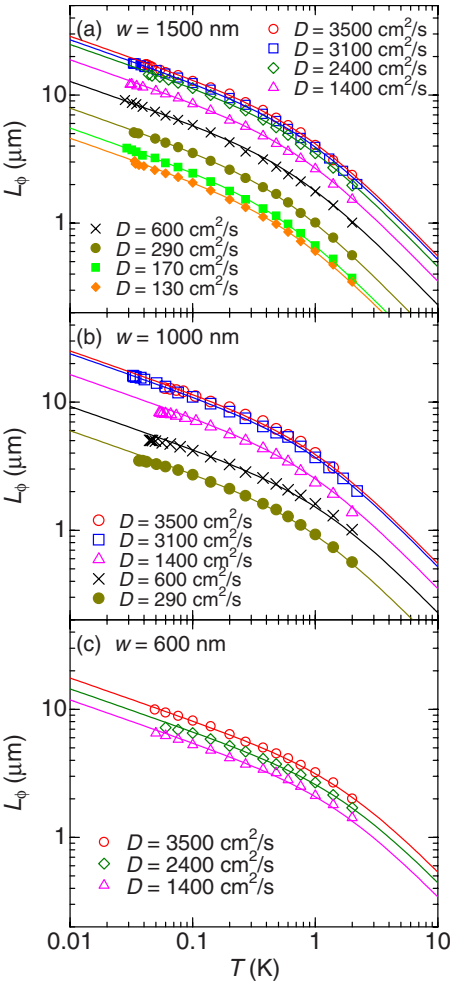

FIG. 14. (Color online) Phase coherence length L_ϕ of three different wires as a function of T at several different diffusion coefficients. The open and solid symbols correspond to the semiballistic regime and the diffusive one, respectively. The solid lines are the best fits to Eq. (8).

V. DISORDER EFFECT ON PHASE COHERENCE

A. Experimental results on quasi-1D wires

In Secs. III and IV, we have been discussing the temperature dependence of the decoherence in the diffusive as well as the semiballistic regimes. In this section, we will discuss the disorder dependence of the decoherence time. For this purpose, we first present in Fig. 14 the temperature dependence of the phase coherence length L_ϕ for three different wire widths and for all investigated diffusion coefficients. Interestingly, the temperature dependence in the low-temperature regime is identical for the diffusive regime and semiballistic regime. Inspecting Fig. 14 more closely, it is clear that the phase coherence length L_ϕ in the semiballistic regime depends more weakly on D compared to the diffusive regime. This can be emphasized by plotting the value of L_ϕ as a function of D at fixed temperature (we take T=60 mK) as shown in Fig. 15. One clearly observes two different D dependencies. In the diffusive regime ($w_{\rm eff} > l_e$), L_ϕ follows a $D^{2/3}$ law, which is consistent with the "standard" model of

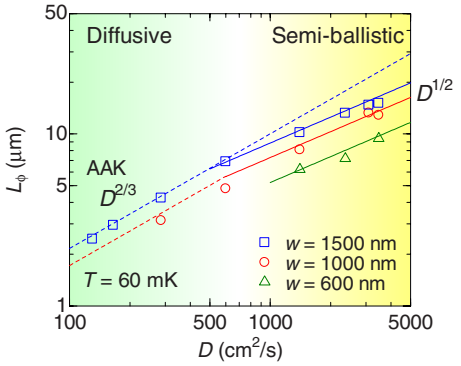

FIG. 15. (Color online) The diffusion coefficient dependence of the phase coherence length L_ϕ at T=60 mK of the three different wires. The broken and solid lines show $D^{2/3}$ and $D^{1/2}$ laws, respectively.

decoherence proposed in the AAK theory[1] [see Eq. (3)]. On the other hand, in the semiballistic regime where $w_{\rm eff} < l_e$, L_ϕ has a different power law as a function of the diffusion coefficient, D^λ with a parameter λ close to 1/2. This behavior can be seen for the three different widths of the wires. The crossover between the two regimes occurs when $w_{\rm eff}$ becomes comparable to l_e, i.e., $D \sim 1000$ cm^2/s.

To compare our experimental results directly with theoretical expressions, it is more convenient to plot the diffusion coefficient dependence of τ_ϕ rather than L_ϕ.[1,3,4] We thus obtain the phase coherence time τ_ϕ assuming that the relation $L_\phi = \sqrt{D\tau_\phi}$ holds for all the investigated diffusion coefficients. In Fig. 16, we show the temperature dependence of the phase coherence time τ_ϕ of the 1500 nm wide wires at different D. At low temperatures, it follows a $T^{-2/3}$ power law at any diffusion coefficient as expected for the quasi-1D diffusive regime [see Eq. (1)]. Above 1 K, τ_ϕ tends towards a T^{-2} dependency, in accordance with the FL theory without disorder [see Eq. (5)].

To make a quantitative analysis, we plot in Fig. 17 the experimental parameter $a_{\rm exp}$ of Eq. (8), normalized by the theoretical prefactor $\alpha_{\rm AAK}$ of Eq. (2), as a function of D.[55] In the diffusive regime, the parameter $a_{\rm exp}/\alpha_{\rm AAK}$ follows a power law as a function of D with $a_{\rm exp}/\alpha_{\rm AAK} \propto D^{-1/3}$, which is consistent with Eq. (2). Moreover, the prefactor $a_{\rm exp}$ obtained in this work agrees with Eq. (3) in absolute value within 15%. In the semiballistic regime, on the other hand, we obtain a very different behavior of $a_{\rm exp}/\alpha_{\rm AAK}$ as a function of D. While in the diffusive regime the parameter $a_{\rm exp}/\alpha_{\rm AAK}$ is in accordance with the diffusive theory, in the semiballistic regime the decoherence time seems to be *independent* of the disorder. On the other hand, we observe the same width dependence of prefactor $a_{\rm exp} \sim w^{-2/3}$ as in the diffusive regime. From these experimental facts, it is obvious that the temperature and width dependence of the phase coherence time τ_ϕ in the semiballistic regime are well captured within the AAK theory, whereas the disorder dependence of τ_ϕ has to be reconsidered in the semiballistic regime.

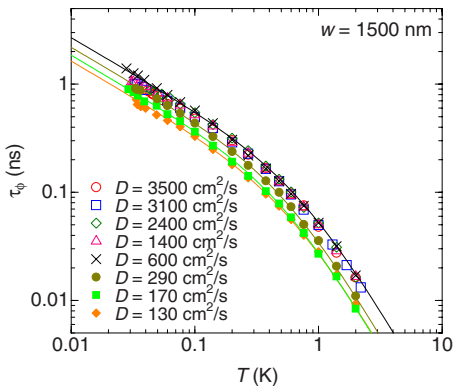

FIG. 16. (Color online) Phase coherence time τ_ϕ of 1500 nm wide wires as a function of T at different diffusion coefficients.

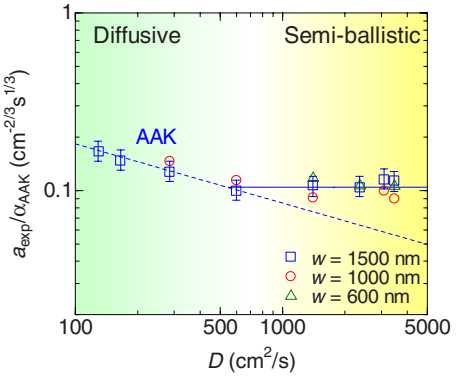

FIG. 17. (Color online) The experimental coefficient $a_{\rm exp}$ of Eq. (8) scaled by $\alpha_{\rm AAK}$ as a function of D. The dashed line represents $D^{-1/3}$.

One could argue that the *disorder-independent* decoherence time in the semiballistic regime might be simply due to saturation of the diffusion coefficient D. If the boundary scattering in quasi-1D wires were diffusive, the diffusion coefficient should saturate at $D = 1/2(v_F w_{\rm eff})$,[49] which could lead to a *D-independent* τ_ϕ. This possibility, however, can be ruled out by plotting the resistance of the wires as a function of D. Figure 18 shows the residual resistance of the quasi-1D wires $R_{\rm res}$ (see Eq. (12) in Sec. VI) as a function of D obtained from the Hall bar.[56] The residual resistance $R_{\rm res}$ nicely follows a $1/Dw_{\rm eff}$ law over the whole D range (see Table I). This dependency can be realized only when the boundary

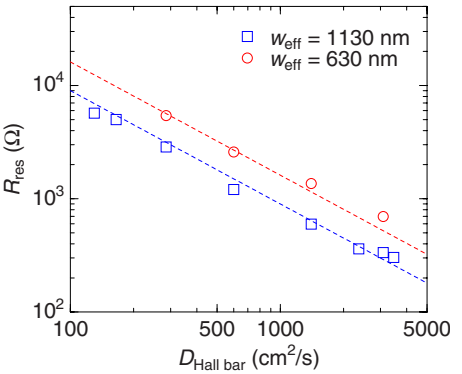

FIG. 18. (Color online) Residual resistance of the wires as a function of D obtained from the Hall bar. The broken lines (blue and red) show $R_{\rm res} \propto 1/Dw_{\rm eff}$ for $w_{\rm eff}$=1130 nm and 630 nm, respectively.

scattering in the semiballistic regime is specular. Moreover, as mentioned in Sec. IV B, our wires have been made by shallow etching which results in highly specular boundary reflection.[25] The D dependence of the residual resistance also confirms our assumption that $L_\phi = \sqrt{D\tau_\phi}$ is valid even in the semiballistic regime.

There is no theoretical prediction about the disorder dependence of the decoherence for quasi-1D wires in the clean limit (very few impurities). There are, however, a few theoretical works to give us some hints. It should be noted that these calculations have been performed for 2D systems. Wittmann and Schmid[57] calculated the 2D WL correction for arbitrary number of elastic scattering time τ_e. They found that the WL correction in the clean limit can be reduced compared to the diffusive case, leading to an underestimation of τ_ϕ. Narozhny *et al.*[54] calculated the temperature dependence of τ_ϕ in a 2D system at arbitrary relation between $k_B T$ and $\hbar/\tau_e$. They showed that the phase coherence time τ_ϕ has the same temperature dependence both in the diffusive and ballistic regimes but the prefactor in the ballistic regime is smaller than in the diffusive one. These theoretical calculations are qualitatively consistent with our experimental result on the quasi-1D wires; as is shown in Fig. 17, the dephasing time τ_ϕ in the semiballistic regime is independent of D while τ_ϕ in the diffusive regime is quantitatively consistent with the AAK theory, i.e., $\tau_\phi \propto D^{1/3}$. However, it is not possible to make a quantitative analysis of the diffusion coefficient dependence of τ_ϕ on the basis of these calculations. It is desirable that theoretical calculations of τ_ϕ in the semiballistic regime are performed for the quasi-1D wires.

B. Comparison with theory on zero-temperature decoherence

As pointed out in Sec. I, decoherence in metallic systems at zero temperature has been a controversial issue over the last decade.[1–24] By studying only the temperature dependence of the phase coherence time it is very difficult to discriminate experimentally whether a saturating decoherence time is observed or not. Firstly, several precautions have to be taken such that an experimentally observed saturation is not caused by either external radio frequency propagating along the measuring lines or by the determination of the actual electron temperature of the sample which is not always straightforward. Secondly, even if all these requirements are fulfilled, a small inclusion of magnetic impurities will always lead to a saturating decoherence time at very low but finite temperature.[10,12,13] In addition, to avoid magnetic impurities in metallic systems is extremely difficult as metallic sources cannot be purchased with a guaranteed impurity level below the parts per million level. It is hence clear that simply studying the temperature dependence is not sufficient to give a definite answer to the saturation problem. A different approach to this problem can be done by studying the diffusion coefficient dependence of the decoherence time. Compared to the AAK theory, the GZ theory predicts a much stronger diffusion coefficient dependence of τ_ϕ at very low temperatures[58] as detailed below. This can be tested with the present experiment.

According to the GZ theory, $\tau_\phi(T)$ intrinsically saturates at zero temperature in the ground state of a disordered conductor at a finite value τ_ϕ^0 due to the fluctuations of the electromagnetic field generated by an electron and which is experienced by the other electrons.[3,4] The finite value depends strongly on the intrinsic disorder. In particular, the GZ theory predicts that $\tau_\phi^0 \propto D^2$ for 2D and $\tau_\phi^0 \propto D$ for 1D.[59,60] Note that the dimensionality here is determined in terms of l_e; the former case should be applied in the diffusive regime where $L, w > l_e$ while the latter case should be applied in the semiballistic regime where $L > l_e > w$.[61] The AAK theory, on the other hand, predicts a very slow D dependence of the dephasing time, i.e., $\tau_\phi \propto D^{1/3}$, as shown in Eq. (3).

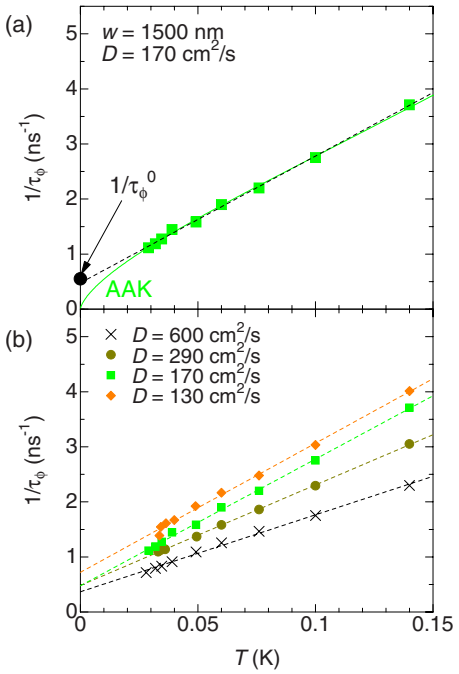

FIG. 19. (Color online) (a) An example to extract $1/\tau_\phi^0$ proposed by GZ (Ref. 60). The solid line shows the best fit of the AAK formula, Eq. (1). The broken line is a linear fit of the dephasing rate $1/\tau_\phi(T)$. The intercept represents $1/\tau_\phi^0$. (b) Dephasing rate $1/\tau_\phi$ at different D as a function of T on a linear scale ($w = 1500$ nm). The broken lines have the same meaning as in (a).

The fact that we do not see any apparent saturation in the temperature dependence of τ_ϕ or L_ϕ for all samples investigated (see Fig. 14) seems already in contradiction with the GZ theory. Nevertheless, we will adopt the method proposed in Ref. 60 to extract the saturation time τ_ϕ^0. This can be done by plotting the inverse of the dephasing time (dephasing rate) as a function of temperature on a linear scale. By extrapolating a linear fit to the low-temperature data down to zero temperature (in our case we take all the data below 150 mK for the fitting), one obtains τ_ϕ^0 as shown in Fig. 19. For comparison we also plot the theoretical expectation within the AAK theory. We then determine τ_ϕ^0 in the same way for all diffusion coefficients investigated. This is shown in Fig. 20 for three wires with different width as well as for the Hall bars. For our data we obtain a very weak variation in τ_ϕ^0 as a function of diffusion coefficient. It is clear that the diffusion coefficient dependence of τ_ϕ^0 is much weaker than the one expected within the GZ theory (dotted and dashed-dotted lines). One could of course argue that our measurements do

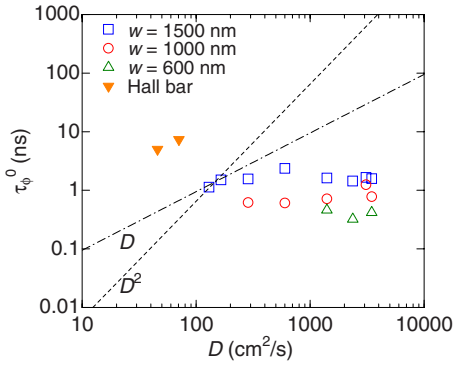

FIG. 20. (Color online) τ_ϕ^0 for all the investigated samples. The dotted and dashed-dotted lines show D^2 and D laws, respectively.

not extend to low enough temperature and that the saturation of τ_ϕ will only occur at lower temperature. This contrasts however with the fact that for metals with similar diffusion coefficients very frequently a saturation of τ_ϕ is observed at much higher temperatures. These facts therefore suggest that the frequently observed low-temperature saturation of τ_ϕ is *not* intrinsic.

VI. TEMPERATURE DEPENDENCE OF THE RESISTANCE

As mentioned above, an important issue in this paper is decoherence at zero temperature. For decoherence measurements at very low temperatures, it is important to know the actual electron temperature of the sample which can be quite different than that of the thermal bath. In order to probe the electron temperature of the 2DEG *in situ*, we have used the temperature dependence of the Altshuler-Aronov correction term as detailed in Sec. VI A.

A. Altshuler-Aronov correction

In the diffusive regime, the electrical resistance of a quantum wire (or Hall bar) consists of different contributions

$$R(B,T) = R_{\text{res}} + R_{\text{e-ph}}(T) + \Delta R_{\text{WL}}(B,T) + \Delta R_{\text{AA}}(T) + \cdots . \tag{12}$$

The first term R_{res} corresponds to the residual resistance and the second term comes from the e-ph interactions. At high temperatures $R_{\text{e-ph}}$ simply follows a T-linear dependence and vanishes as temperature goes to zero. The third term is the WL quantum correction term, which has already been described in Sec. III A. The last term is the so-called Altshuler-Aronov (AA) correction.[62] At low temperatures, the e-e interactions are responsible for a small depletion of the density of states at the Fermi energy which leads to a correction to the resistivity. Basically, the WL and AA corrections are of the same order but the latter can be distinguished from the former by applying a small magnetic field which suppresses the WL correction. The AA correction in the quasi-1D case is given as below

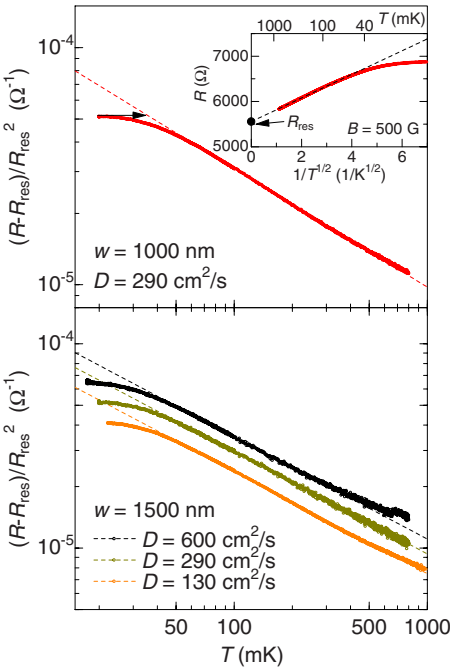

FIG. 21. (Color online) Resistance variations in 1000 (top) and 1500 nm wide wires (bottom) as a function of T at B=500 G and 300 G, respectively. The broken lines are the best fits of Eq. (13). The *real electron temperature* below 40 mK is corrected by the $1/\sqrt{T}$ law (see the arrow). In the inset of the top figure, the resistance of 1000 nm wide wires is plotted as a function of $1/\sqrt{T}$ to extract R_{res}.

$$\Delta R_{\text{AA}}(T) \equiv R(T) - R_{\text{res}} = 0.782\lambda_\sigma R_{\text{res}}^2 N \frac{e^2}{h}\frac{L_T}{L} = R_{\text{res}}^2 \frac{A_{\text{theo}}}{\sqrt{T}} . \tag{13}$$

The parameter λ_σ is a constant, which represents the strength of the screening of the interactions. In the quasi-1D case, one has $\lambda_\sigma = 4 - 3F/2$, where F is the screening factor varying from 0 for an unscreened interaction to 1 for a perfectly screened interaction. In a similar manner, one can obtain the 2D AA correction in the limit $T < \hbar/(k_B\tau_e)$,

$$\Delta R_{\text{AA}}(T) = \lambda_\sigma R_{\text{res}}^2 \frac{e^2}{2\pi h}\frac{w}{L}\left\{\gamma - \ln\left(\frac{2\pi k_B T \tau_e}{\hbar}\right)\right\}, \tag{14}$$

where $\gamma \simeq 0.577$ is the Euler constant and $\lambda_\sigma = 2 - 3F/2$.

B. Experimental results in the diffusive regime

At fields high enough to suppress the WL correction (B=150–500 G), the resistance of a quasi-1D metallic wire follows a $1/\sqrt{T}$ law due to electron-electron interactions and can be used as a "thermometer" to probe the *effective electron temperature*.[10] For this purpose, we plot the resistance of our 1000 nm wide wire as a function of $1/\sqrt{T}$ in the inset of Fig. 21. It follows nicely the $1/\sqrt{T}$ dependence down to 40 mK.[63] Below this temperature it starts to deviate from the $1/\sqrt{T}$ law. This is also observed for wires with different widths and different diffusion coefficients. To show the deviation more clearly, $(R - R_{\text{res}})/R_{\text{res}}^2$ is plotted as a function of

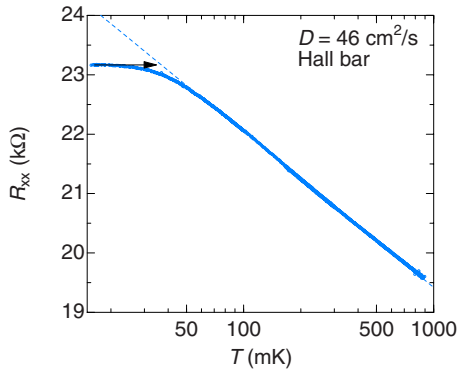

FIG. 22. (Color online) Resistance variation in the Hall bar at $D=46$ cm^2/s as a function of T. The broken line shows a $\ln(T)$ law.

temperature in Fig. 21, where R_{res} is obtained by extrapolating the R vs $1/\sqrt{T}$ curve down to zero (see inset of Fig. 21). Assuming that the $1/\sqrt{T}$ dependence of the resistance holds down to the lowest temperature, we obtain an effective electron temperature of 25 mK at the base temperature of our cryostat. This fact is also confirmed by the temperature dependence of the phase coherence length (see Fig. 7). Therefore, all our data have been temperature corrected below 40 mK.

In Fig. 22, the resistance variation in the 2D Hall bar for $D=46$ cm^2/s is plotted as a function of T on a semilog scale. As expected from Eq. (14), the AA correction term follows a $\ln(T)$ law down to 40 mK. Like in the case of quasi-1D wires, below this temperature the resistance deviates from the theoretical expression. In a similar manner we correct the actual temperature below 40 mK.

C. Experimental results in the semiballistic regime

In the semiballistic regime where $l_e > w_{\mathrm{eff}}$, we find an unexpected temperature dependence of the resistance. In Fig. 23, a resistance vs $1/\sqrt{T}$ curve in this regime

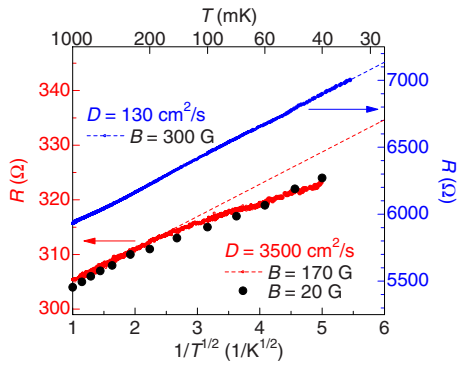

FIG. 23. (Color online) Resistance of 1500 nm wide wires as a function of $1/\sqrt{T}$ at $D=3500$ (left axis) and 130 cm^2/s (right axis). The resistance at $D=130$ cm^2/s is measured at $B=300$ G ($B/B^*=0.07$) while the resistance at $D=3500$ cm^2/s is measured at $B=20$ ($B/B^*=0.12$; black dots) and 170 G ($B/B^*=1$; red curve). The broken lines are linear fits to extract R_{res}. The temperature below 40 mK has already been corrected for both diffusion coefficients.

($D=3500$ cm^2/s) is compared to that in the diffusive regime (130 cm^2/s). As discussed above, in the diffusive regime and at fields high enough to suppress WL the resistance follows nicely a $1/\sqrt{T}$ law in the entire temperature range. In the semiballistic regime, on the other hand, we observe a deviation from the $1/\sqrt{T}$ law below 150 mK which is somewhat unexpected.

In this regime one has to be careful about the applied magnetic field to suppress WL such that it does not affect the trajectories of the electrons, in other words, does not lead the SdH oscillations. According to Ref. 64, the AA correction to resistance is independent of B when the condition $B/B^* \ll 1$ is satisfied. We have therefore measured the e-e interaction correction for different magnetic fields as shown in Fig. 23. For fields lower than 170 G ($B/B^*=1$) we do not observe a significant change in the temperature dependence and we can rule out the possibility that the observed temperature dependence is due to the applied magnetic field. It is also unlikely that the observed temperature dependence is due to a decoupling of the electrons from the thermal bath since the phase coherence length nicely follows the AAK theory down to the lowest temperatures as shown in Fig. 14. We also exclude the possibility that this temperature dependence results from a dimensional crossover when the thermal length $L_T=\sqrt{\hbar D/k_B T}$ becomes comparable to the width of the wire w_{eff}.[63]

When entering the semiballistic regime ($l_e > w_{\mathrm{eff}}$), as the scattering at the boundaries in our wires is mostly specular, the temperature dependence of the e-e interactions may be influenced[65,66] and modified by an additional logarithmic term at intermediate temperatures ($k_B T\tau_e/\hbar \approx 1$).

In the following, we will try to fit the observed temperature dependence of the e-e interaction correction by a combination of a $1/\sqrt{T}$ and a logarithmic term

$$\frac{\Delta R_{\mathrm{AA}}(T)}{R_{\mathrm{res}}^2} = \frac{A_{\mathrm{exp}}}{\sqrt{T}} + B_{\mathrm{exp}} \ln(T). \tag{15}$$

This is shown in Fig. 24. Indeed, fitting with Eq. (15) reproduces fairly well the observed temperature dependence in the semiballistic regime (see dashed-dotted lines in Fig. 24). Deep in the semiballistic regime, we see a relatively strong deviation from the $1/\sqrt{T}$ dependence. By decreasing the diffusion coefficient, the temperature dependence becomes more and more 1D like and turns completely into the 1D regime when entering the diffusive regime ($l_e < w_{\mathrm{eff}}$). From fitting the data with Eq. (15) we can extract the values of the prefactors of the 1D (A_{exp}) as well as logarithmic behavior (B_{exp}) as shown in Fig. 25. We observe that the prefactor of the 1D contribution is proportional to $D^{1/2}$ as expected from Eq. (13). In addition, A_{exp} shows no wire width dependence, which is consistent with Eq. (13). In the diffusive regime ($D<1000$ cm^2/s), the logarithmic contribution is negligible. However, when entering the semiballistic regime, the prefactor of the logarithmic contribution becomes comparable to the 1D term and dominates the 1D term for our cleanest samples. In the overall temperature dependence, the additional logarithmic contribution shifts the crossover temperature where the 1D AA behavior dominates to much

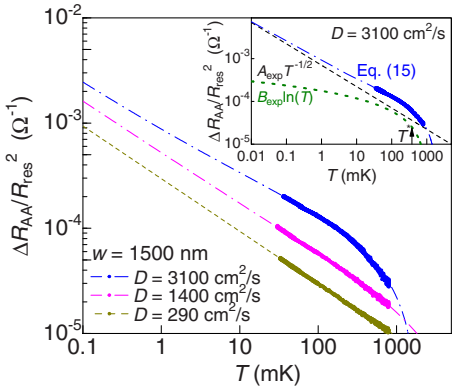

FIG. 24. (Color online) Resistance variations in 1500 nm wide wires as a function of T for three different diffusion constants. The dashed-dotted lines are the best fits to Eq. (15). Inset: resistance variation in the 1500 nm wide wires at $D=3100$ cm^2/s. The broken line (black) shows the $1/\sqrt{T}$ law whereas the dotted line (green) shows the $\ln(T)$ dependence. The dashed-dotted line (blue) is again the best fit to Eq. (15). T^* indicates the temperature where $T^*=\hbar/(\tau_e k_B)$.

lower temperatures. This is in line with the crossover calculated in Ref. 66 where the crossover temperature T^* is renormalized due to the electron-electron interactions.

VII. STRONGLY LOCALIZED REGIME

So far, we have discussed decoherence in the weakly localized regime for quasi-1D wires and 2D Hall bars. In that regime, one has to meet conditions such that the $k_F l_e$ value is much larger than 1 and also the localization length ξ_{loc} is much larger than L_ϕ. By increasing the disorder, however, one can reach a regime where $k_F l_e$ is on the order of 1 and which is usually referred to as the *strongly localized* regime. In this last section we will present measurements of the resistance as well as the phase coherence length in quasi-1D wires and 2D Hall bars in this regime.

A. 2D Hall bars

For the 2D case a fair amount of experimental[67–77] as well as theoretical works[78–83] can be found in the literature. It is

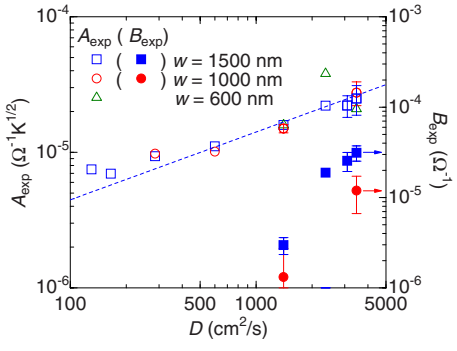

FIG. 25. (Color online) The experimental prefactors A_{exp} (left axis) and B_{exp} (right axis) of the AA correction as a function of D. The broken line shows a $D^{1/2}$ law.

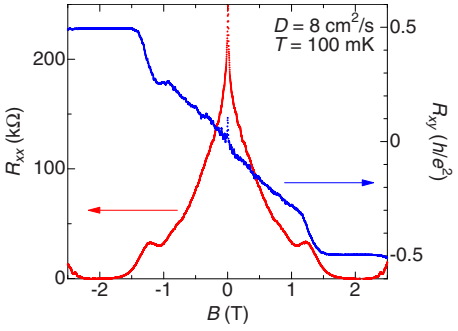

FIG. 26. (Color online) R_{xx} and R_{xy} at $D=8$ cm^2/s and $T=100$ mK. The Hall resistance R_{xy} is normalized by h/e^2.

commonly believed that the conduction process in the strongly localized regime is attributable to 2D variable range hopping and several experiments support this assumption.[69–72] On the contrary, the question on how decoherence is affected when going from the *weakly localized* to the *strongly localized* regime is still open.

This problem has been studied mainly in semiconductor heterojunctions with 2DEGs.[69–77] In such 2D systems, an estimation of the localization length ξ_{loc}^{2D} is given by[74,75]

$$\xi_{loc}^{2D} = l_e \exp\left(\frac{\pi}{2} k_F l_e\right) = \frac{2\sqrt{2\pi}m^*}{\sqrt{nh}} D \exp\left(\frac{2\pi^2 m^*}{h} D\right). \tag{16}$$

When ξ_{loc}^{2D} becomes comparable or smaller than the phase coherence length L_ϕ, one enters the strongly localized regime.

In Fig. 26 we show R_{xx} and R_{xy} at $k_F l_e=0.95$ (or $D=8$ cm^2/s) at $T=100$ mK. At $B\sim 2$ T, we can still observe the $\nu=2$ quantum plateau where $R_{xx}=0$. At low fields, R_{xx} shows a large negative magnetoresistance which is more than ten times larger than h/e^2 for $B=0$. In order to see how R_{xx} evolves with temperature in the low-field region, we plot the magnetoresistance for different temperatures on a semilog plot in Fig. 27(a). With decreasing temperature, the peak height exponentially grows but the shape of the magnetoresistance seems to be similar to that in the weakly localized regime down to $T\sim 100$ mK (see Fig. 8). Below this temperature, R_{xx} near zero field is extremely enhanced. Such a *large* negative magnetoresistance is probably a precursor of the $\exp(-\sqrt{B})$ law expected in the model of interference effects in variable range hopping.[83] Let us now discuss in more detail the temperature dependence of the resistance at zero field and at a field of 2000 G where the WL correction is basically suppressed. As seen in Fig. 27(b), above 1 K R_{xx} follows a $\ln(T)$ dependence as expected in the weakly localized regime (see Fig. 22). Below 1 K, R_{xx} deviates from the $\ln(T)$ law and can be fitted to a 2D variable range hopping law $R(T)\propto\exp(T_M/T)^{1/3}$; $T_M=300$ and 28 mK for 0 G and 2000 G, respectively. Such a behavior has already been seen in other experiments in the strongly localized regime.[69–72]

As pointed out above, the shape of the magnetoresistance is similar to that in the weakly localized regime. Although the WL theory Eq. (7) is, in principle, only applicable in the

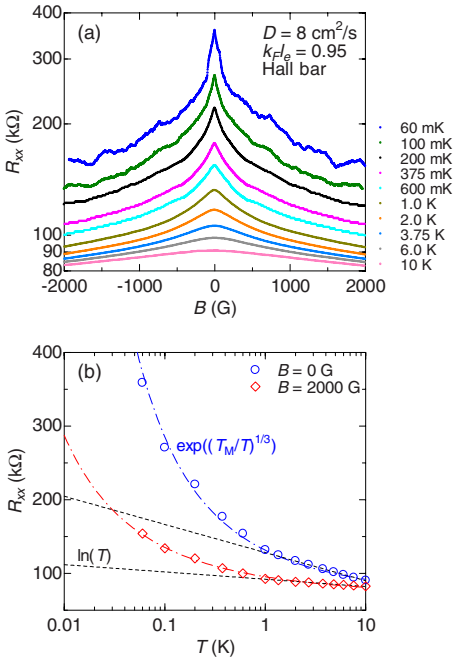

FIG. 27. (Color online) (a) Magnetoresistance curves of the Hall bar at $D=8$ cm^2/s at several different temperatures. (b) R_{xx} at $B=0$ and 2000 G as a function of temperature. The broken and dashed-dotted lines represent ln(T) and 2D variable range hopping laws, respectively.

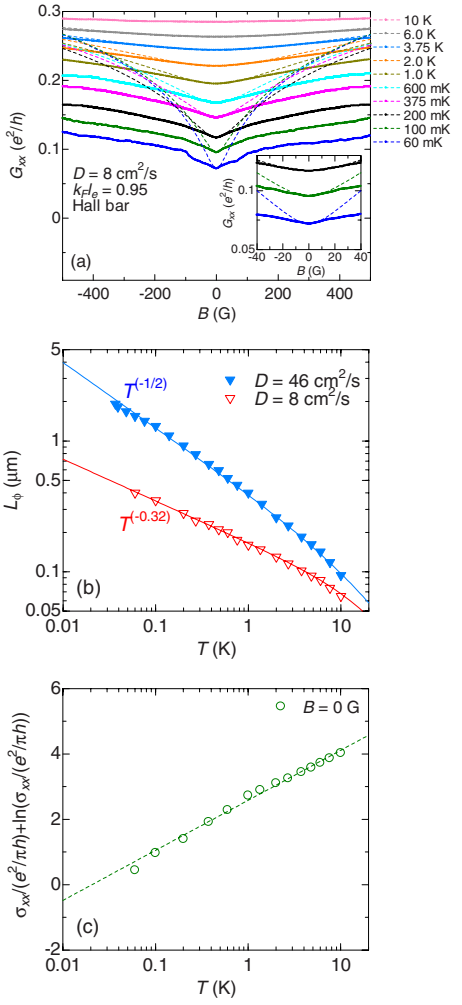

FIG. 28. (Color online) (a) Magnetoconductance curves of the Hall bar at $D=8$ cm^2/s at several different temperatures. The conductance is divided by e^2/h. The broken lines show the best fits of Eq. (7). The inset shows a closeup view of the low-field part of the magnetoconductance at low temperatures. (b) Temperature dependence of L_ϕ in the strongly localized regime (open symbols). For comparison, L_ϕ in the weakly localized regime (closed symbols) is also plotted. (c) Temperature dependence of σ_{xx} in the representation corresponding to the self-consistent theory, Eq. (17).

weakly localized regime, we nevertheless fit the magnetoconductance curves with Eq. (7) as shown in Fig. 28(a) at temperatures higher than 60 mK. A similar approach has already been done by Minkov *et al.*[73,75] Let us recall that Eq. (7) is limited to a small field range within $B_c=\hbar/4eL_\phi^2$. At high temperatures, the fitting works very well in a relatively wide field range. Going to lower temperatures, the fitting region is getting smaller which indicates that L_ϕ increases. The obtained L_ϕ from the WL theory is plotted as a function of T in Fig. 28(b). The phase coherence length L_ϕ of the Hall bar in the *strongly* localized regime follows a power law T^p at low temperatures as indicated by the solid line, just like in the weakly localized regime, but with a smaller exponent $p=-0.32$. Such a temperature dependence is very similar to what has been observed in Ref. 74 for similar values of $k_F l_e$. In that work,[74] the exponent varied from $p=-0.5$ to -0.3 when reducing $k_F l_e<5$ down to $k_F l_e \sim 1$, similar to our observations.

Within the theoretical approach of the phase coherence in the Anderson localization regime proposed by Vollhardt and Wölfle,[79,82] the conductivity can be calculated for arbitrarily weak disordered systems. Their self-consistent theory leads to the following equation for the conductivity $\sigma_{xx}(T)$:[73]

$$\left\{\frac{\sigma_{xx}(T)}{(e^2/\pi h)}+\ln\left[\frac{\sigma_{xx}(T)}{e^2/\pi h}\right]\right\}=\pi k_F l_e+\ln(\pi k_F l_e)-2\ln\left[\frac{L_\phi(T)}{l_e}\right], \quad (17)$$

where we assume that $L_\phi=\sqrt{D\tau_\phi}$ and $L_\phi \gg l_e$. Strictly speaking, Eq. (17) is valid only when $k_F l_e \gg 1$. Nevertheless, inspired by Ref. 73, we plot the left side of Eq. (17) for $B=0$ G as a function of T in Fig. 28(c). It exhibits a ln(T) dependence over the whole temperature range.[84] Such a ln(T) law is expected if one assumes a power law for the temperature dependence of the phase coherence length. From the slope of the left side of Eq. (17) vs T curve, we can determine the exponent of $L_\phi(T)$ [$L_\phi(T) \propto T^p$]. Interestingly, we again obtain $p \simeq -0.32$ which is identical to the one obtained when fitting the temperature dependence of the magnetoconductance with the WL theory [see Fig. 28(b)]. This hints to the conclusion that when going from the weakly localized to the strongly localized regime the temperature dependence of L_ϕ is still diverging with decreasing temperature with a power law but with a smaller exponent compared to the weakly localized regime.

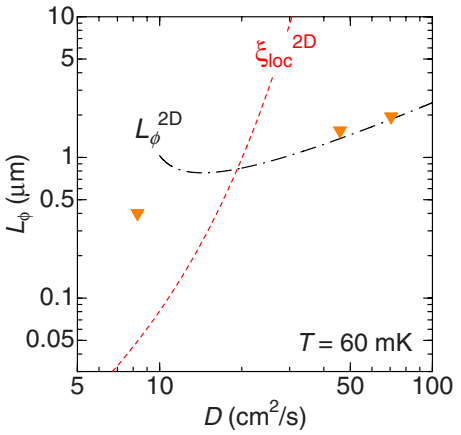

FIG. 29. (Color online) Phase coherence length L_ϕ of Hall bars at T=60 mK as a function of D. The broken and dashed-dotted lines represent the 2D localization length, Eq. (16), and theoretically expected phase coherence length L_ϕ^{2D} based on Eq. (4), respectively.

Before closing this section, let us mention the diffusion coefficient dependence of the phase coherence length in 2D systems. In Fig. 29, we plot L_ϕ obtained at T=60 mK in 2D Hall bars as a function of D. In the weakly localized regime, L_ϕ nicely follows the formula based on Eq. (4) as shown in the dashed-dotted line in Fig. 29. With decreasing D, this formula diverges because of the logarithmic term in Eq. (4),[85] and the 2D localization length ξ_{loc}^{2D} becomes smaller than the phase coherence length. In the strongly localized regime at zero temperature electrons should be localized within a length scale of ξ_{loc}^{2D}. At finite temperatures, on the other hand, they can hop from one island with a size of ξ_{loc}^{2D} to another, and this hopping process gives rise to the exponential increase in the resistance as shown in Fig. 27(b). During this process the phase coherence of the electrons should be maintained within a length scale of L_ϕ. Thus, in the strongly localized regime, the phase coherence length L_ϕ can be larger than the localization length ξ_{loc}^{2D}.

B. 1D wires

In the case of quasi-1D wires, the localization length ξ_{loc}^{1D} depends on the effective width of the wires and the diffusion coefficient as below[86,87]

$$\xi_{loc}^{1D} = \frac{k_F l_e}{\pi} w_{eff} = \frac{4m^*}{h} w_{eff} D. \quad (18)$$

Since L_ϕ varies proportionally to $D^{2/3}$ in the diffusive regime, L_ϕ can be fine tuned such that it becomes close to ξ_{loc}^{1D}. For the case of our wires this should occur in the diffusion coefficient range from D=30 to 300 cm^2/s for T=25 mK. This is shown in Figs. 30(a)–30(c), where we plot the theoretical localization length ξ_{loc}^{1D} as well as the expected phase coherence length L_ϕ^{AAK} at our lowest temperature

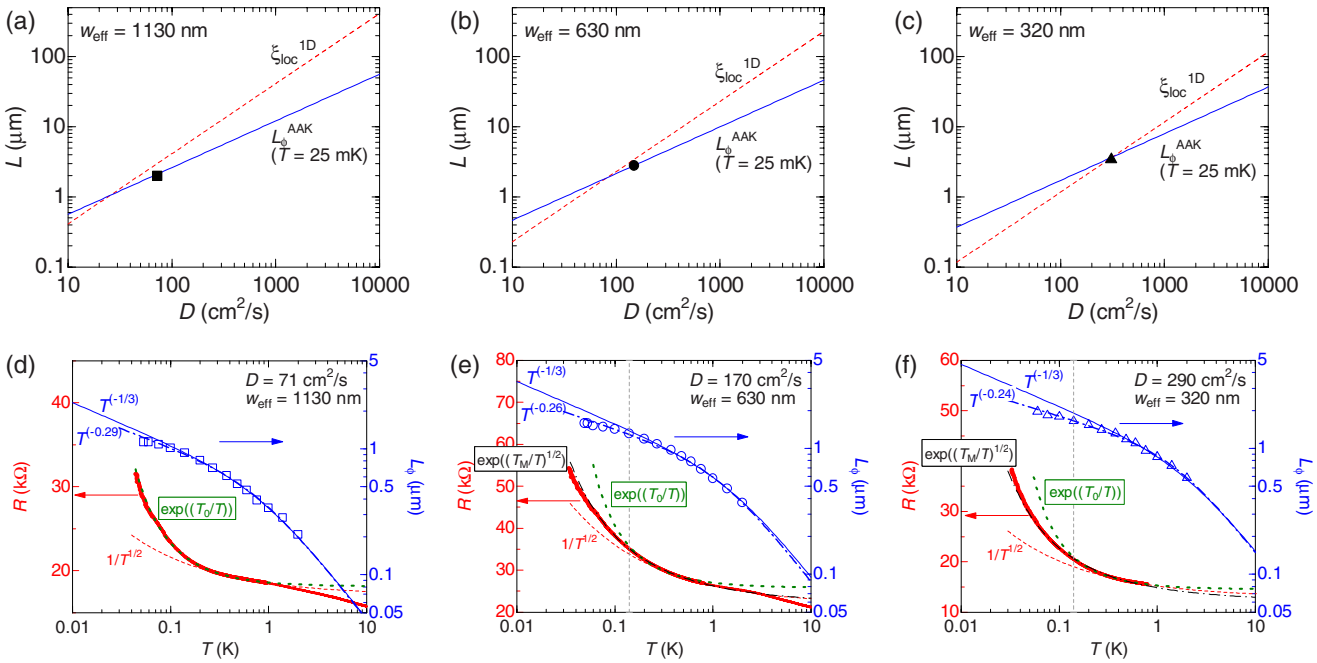

FIG. 30. (Color online) [(a)–(c)] Diffusion coefficient dependence of the theoretical 1D localization length, Eq. (18), and phase coherence length expected in the AAK theory at T=25 mK; (a) w_{eff}=1130, (b) 630, and (c) 320 nm. The closed symbols represent the diffusion coefficient where the $R(T)$ and L_ϕ measurements have been performed. [(d)–(f)] Experimental data of $R(T)$ (red solid lines) and L_ϕ (blue open symbols) as a function of T; (d) w_{eff}=1130, (e) 630, and (f) 320 nm. The solid lines for $L_\phi(T)$ are the best fits of Eq. (8). For the dashed-dotted lines, we have changed the exponent of $L_\phi(T)$ at the low-temperature part from −1/3 (AAK) to −0.29 (w_{eff}=1130 nm), −0.26 (w_{eff}=630 nm), or −0.24 (w_{eff}=320 nm) in order to get better fitting precisions down to lower temperatures. The broken, dotted, dashed-dotted lines for $R(T)$ show the best fits of $1/\sqrt{T}$, $\exp(T_0/T)$, and $\exp[(T_M/T)^{1/2}]$ laws, respectively. The vertical dotted lines in (e) and (f) represent the temperatures below which $L_\phi(T)$ and $R(T)$ deviate from the AAK theory, Eq. (8), and from the activation law Eq. (19), respectively.

TABLE III. Fitting parameters of the activation and 1D variable range hopping laws.

w_{eff} (nm)	D (cm^2/s)	T_0 (mK)	T_M (mK)	T_ξ (mK)
1130	71	25		9
630	170	45	30	12
320	290	51	39	28

$T=25$ mK as a function of D for three different widths of the wires.

In Figs. 30(d)–30(f), we show the temperature dependence of measured $R(T)$ and L_ϕ. Here, L_ϕ has been obtained again by fitting the magnetoconductance to the WL theory.[88] Above 200 mK, the resistance of the wires still follows a $1/\sqrt{T}$ law which is attributable to the AA correction in the diffusive regime. Below this temperature, the resistance deviates from the $1/\sqrt{T}$ law and diverges exponentially. On the other hand, the phase coherence length L_ϕ follows again a power law, but with an exponent smaller compared to the diffusive regime [see dashed-dotted line for $L_\phi(T)$ in Fig. 30]. The qualitative behavior is indeed similar to the 2D case.

The exponential divergence of $R(T)$ can be fitted to different exponential laws, like the simple activation law[89]

$$R(T) \propto \exp(T_0/T) \tag{19}$$

or the 1D variable range hopping law

$$R(T) \propto \exp\{(T_M/T)^{1/2}\}. \tag{20}$$

For instance, $R(T)$ for $w_{\mathrm{eff}}=1130$ nm wide wires nicely follows Eq. (19) down to the lowest temperature,[90] whereas the variable range hopping does not give satisfactory results. On the other hand, for $w_{\mathrm{eff}}=630$ and 320 nm wide wires, it can also be fitted by the activation law, Eq. (19), down to ~ 150 mK, but the 1D variable range hopping law, Eq. (20), gives better fitting precisions down to lower temperatures. The two fitting parameters T_0 in Eq. (19) and T_M in Eq. (20) are listed in Table III.

Similar behavior of $L_\phi(T)$ and exponential divergence of resistance in quasi-1D conductors have already been reported by Gershenson and co-workers.[86,91] They claim that (i) the exponential divergence of resistance is due to the activation law, (ii) the crossover temperature T_ξ where $L_\phi^{\mathrm{AAK}}(T_\xi)=\xi_{\mathrm{loc}}^{\mathrm{1D}}$ is close to T_0, and (iii) L_ϕ deviates (saturates) at certain temperature (T_{dev}) as the temperature approaches T_0. These observations are *qualitatively* consistent with our experimental data. However, we observe clear *quantitative* disagreement among the three different temperatures T_ξ, T_{dev}, and T_0 which are more or less similar in Refs. 86 and 91. It is therefore highly desirable to investigate theoretically the detailed mechanisms of L_ϕ and $R(T)$ in quasi-1D conductors near the crossover point from the weakly localized to strongly localized regime.

In this section, we have confirmed that in the strongly localized regime the phase coherence time is diverging with a power law at low temperatures. The exponent is reduced compared to the weakly localized regime when the system approaches the strongly localized regime. Let us remind, however, that for the extraction of the exponent we applied the WL formula in a regime where it should, in principle, not be valid. On the other hand, our data seems to show that the WL theory gives a very good description of the magnetoconductance of quasi-1D and 2D mesoscopic conductors beyond the weakly localized regime both in the semiballistic and strongly localized regimes.

VIII. CONCLUSIONS

We have studied the disorder dependence of the phase coherence time τ_ϕ of quasi-1D wires and 2D Hall bars made from a 2D electron gas. By implanting locally gallium ions into the doping layer of the heterostructure using a focused ion beam microscope, we have been able to change the electronic diffusion coefficient D over 3 orders of magnitude. This allowed to explore various physical regimes, namely, the semiballistic, the weakly localized and the strongly localized regimes. In the weakly localized regime, the temperature as well as the diffusion coefficient dependence of the phase coherence time is in extremely good agreement with the "standard model" of decoherence proposed by AAK. In particular, for quasi-1D wires, the diffusion coefficient dependence of the phase coherence time follows a $D^{1/3}$ power law, while the temperature dependence follows a $T^{-2/3}$ power law. Similar observations have been found for the 2D system: the phase coherence time τ_ϕ follows a T^{-1} law as expected within the AAK theory. We do not see any sign of saturation of the phase coherence time down to a temperature of 25 mK. In the semiballistic regime where the elastic mean-free path is larger than the width of the wires, we have found a regime where τ_ϕ is independent of the diffusion coefficient. In this regime, the temperature dependence of τ_ϕ is identical to that of the one observed in the weakly localized regime. In the strongly localized regime, where the resistance diverges exponentially with decreasing temperature, we still observe a diverging phase coherence time, however the exponent of the power law is decreased compared to the weakly localized regime.

ACKNOWLEDGMENTS

We acknowledge helpful discussions with G. Montambaux, C. Texier, J. Meyer, S. Kettemann, A. D. Zaikin, S. Florens, R. Whitney, D. Carpentier, J. V. Delft, O. Yevtushenko, and C. Strunk, and technical help from C. Guttin, P. Chanthib, and T. Fournier. Y.N. acknowledges financial support from the "JSPS Research Program for Young Scientists." This work has been supported by the European Commission FP6 NMP-3 Project No. 505457-1 "Ultra 1D" and the *Agence Nationale de la Recherche* under the grant ANR PNano "QuSpin" as well as BMBF "nanoQUIT" and SFB491.

*Present address: Institute for Solid State Physics, University of Tokyo, Japan.
†bsm@listes.grenoble.cnrs.fr

[1] B. L. Altshuler, A. G. Aronov, and D. E. Khmelnitsky, J. Phys. C **15**, 7367 (1982).
[2] P. Mohanty, E. M. Q. Jariwala, and R. A. Webb, Phys. Rev. Lett. **78**, 3366 (1997).
[3] D. S. Golubev and A. D. Zaikin, Phys. Rev. Lett. **81**, 1074 (1998).
[4] D. S. Golubev and A. D. Zaikin, Phys. Rev. B **74**, 245329 (2006).
[5] Y. Imry, H. Fukuyama, and P. Schwab, Europhys. Lett. **47**, 608 (1999).
[6] A. Zawadowski, J. von Delft, and D. C. Ralph, Phys. Rev. Lett. **83**, 2632 (1999).
[7] F. Pierre and N. O. Birge, Phys. Rev. Lett. **89**, 206804 (2002).
[8] F. Schopfer, C. Bäuerle, W. Rabaud, and L. Saminadayar, Phys. Rev. Lett. **90**, 056801 (2003).
[9] F. Pierre, A. B. Gougam, A. Anthore, H. Pothier, D. Esteve, and N. O. Birge, Phys. Rev. B **68**, 085413 (2003).
[10] C. Bäuerle, F. Mallet, F. Schopfer, D. Mailly, G. Eska, and L. Saminadayar, Phys. Rev. Lett. **95**, 266805 (2005).
[11] G. M. Alzoubi and N. O. Birge, Phys. Rev. Lett. **97**, 226803 (2006).
[12] F. Mallet, J. Ericsson, D. Mailly, S. Ünlübayir, D. Reuter, A. Melnikov, A. D. Wieck, T. Micklitz, A. Rosch, T. A. Costi, L. Saminadayar, and C. Bäuerle, Phys. Rev. Lett. **97**, 226804 (2006).
[13] L. Saminadayar, P. Mohanty, R. A. Webb, P. Degiovanni, and C. Bäuerle, Physica E **40**, 12 (2007).
[14] T. Capron, Y. Niimi, F. Mallet, Y. Baines, D. Mailly, F.-Y. Lo, A. Melnikov, A. D. Wieck, L. Saminadayar, and C. Bäuerle, Phys. Rev. B **77**, 033102 (2008).
[15] M. G. Vavilov, L. I. Glazman, and A. I. Larkin, Phys. Rev. B **68**, 075119 (2003).
[16] G. Zaránd, L. Borda, J. von Delft, and N. Andrei, Phys. Rev. Lett. **93**, 107204 (2004).
[17] L. Borda, L. Fritz, N. Andrei, and G. Zaránd, Phys. Rev. B **75**, 235112 (2007).
[18] T. Micklitz, A. Altland, T. A. Costi, and A. Rosch, Phys. Rev. Lett. **96**, 226601 (2006).
[19] T. Micklitz, T. A. Costi, and A. Rosch, Phys. Rev. B **75**, 054406 (2007).
[20] T. A. Costi, L. Bergqvist, A. Weichselbaum, J. von Delft, T. Micklitz, A. Rosch, P. Mavropoulos, P. H. Dederichs, F. Mallet, L. Saminadayar, and C. Bäuerle, Phys. Rev. Lett. **102**, 056802 (2009).
[21] J. Wei, S. Pereverzev, and M. E. Gershenson, Phys. Rev. Lett. **96**, 086801 (2006).
[22] J. J. Lin and L. Y. Kao, J. Phys.: Condens. Matter **13**, L119 (2001).
[23] M. Noguchi, T. Ikoma, T. Odagiri, H. Sakakibara, and S. N. Wang, J. Appl. Phys. **80**, 5138 (1996).
[24] Y. Niimi, Y. Baines, T. Capron, D. Mailly, F.-Y. Lo, A. D. Wieck, T. Meunier, L. Saminadayar, and C. Bäuerle, Phys. Rev. Lett. **102**, 226801 (2009).
[25] Y. Lee, G. Faini, and D. Mailly, Phys. Rev. B **56**, 9805 (1997), and references therein.
[26] J. F. Ziegler and J. P. Biersack, http://www.srim.org/
[27] For this reason, we did not observe any differences on decoherence between Ga^+ and Mn^+ implanted samples with low doses ($<10^8$ cm^{-2}), although manganese atom is a magnetic impurity.
[28] D. Diaconescu, A. Goldschmidt, D. Reuter, and A. D. Wieck, Phys. Status Solidi B **245**, 276 (2008).
[29] A. D. Wieck and K. Ploog, Surf. Sci. **229**, 252 (1990).
[30] In case of high implantation doses, the implanted ion acts in GaAs predominantly as a double acceptor, which is not the case here.
[31] These temperatures have been chosen so that one can extract the residual resistance R_{res} in Hall bars [i.e., minimize $R_{e\text{-}ph}(T)$ as well as $R_{AA}(T)$] [see Eq. (12) in Sec. VI].
[32] A. Zorin, Rev. Sci. Instrum. **66**, 4296 (1995).
[33] D. C. Glattli, P. Jacques, A. Kumar, P. Pari, and L. Saminadayar, J. Appl. Phys. **81**, 7350 (1997).
[34] In noble metals, the prefactor of the temperature dependence of $1/\tau_{e\text{-}e}(\propto T^{2/3})$ is the same order as that of $1/\tau_{e\text{-}ph}(\propto T^3)$ and the crossover from $1/\tau_{e\text{-}e}$ to $1/\tau_{e\text{-}ph}$ can be seen at around 1 K (Ref. 13). In semiconductors, however, the former can be more than 100 times larger than the latter because of small electron density. In addition, as detailed in Sec. III B, the decoherence time without disorder, Eq. (5), becomes dominant above 1 K. Thus, the crossover from $1/\tau_{e\text{-}e}(\propto T^2)$ to $1/\tau_{e\text{-}ph}(\propto T^3)$ occurs at about 100 K. This is the reason why the decoherence time due to the e-ph interactions in semiconductors can be neglected below 10 K.
[35] H. Fukuyama and E. Abrahams, Phys. Rev. B **27**, 5976 (1983).
[36] The crossover temperature for metals is on the order of 100 K.
[37] F. Schopfer, F. Mallet, D. Mailly, C. Texier, G. Montambaux, C. Bäuerle, and L. Saminadayar, Phys. Rev. Lett. **98**, 026807 (2007).
[38] C. Texier, P. Delplace, and G. Montambaux, Phys. Rev. B **80**, 205413 (2009).
[39] D. Hoadley, P. McConville, and N. O. Birge, Phys. Rev. B **60**, 5617 (1999).
[40] P. Mohanty and R. A. Webb, Phys. Rev. Lett. **91**, 066604 (2003).
[41] L. Saminadayar, C. Bäuerle, and D. Mailly, in *Encyclopedia of Nanoscience and Nanotechnology*, edited by H. S. Nalwa (American Scientific, Valencia, CA, 2004), Vol. 3, pp. 267–285.
[42] E. Akkermans and G. Montambaux, *Mesoscopic Physics of Electrons and Photons* (Cambridge University Press, Cambridge, 2007).
[43] C. W. J. Beenakker and H. van Houten, Solid State Phys. **44**, 1 (1991).
[44] M. Ferrier, L. Angers, A. C. H. Rowe, S. Guéron, H. Bouchiat, C. Texier, G. Montambaux, and D. Mailly, Phys. Rev. Lett. **93**, 246804 (2004).
[45] In this fitting, we neglect the $\ln(T)$ term in Eq. (5).
[46] V. T. Renard, I. V. Gornyi, O. A. Tkachenko, V. A. Tkachenko, Z. D. Kvon, E. B. Olshanetsky, A. I. Toropov, and J.-C. Portal, Phys. Rev. B **72**, 075313 (2005).
[47] M. Eshkol, E. Eisenberg, M. Karpovski, and A. Palevski, Phys. Rev. B **73**, 115318 (2006).
[48] S. McPhail, C. E. Yasin, A. R. Hamilton, M. Y. Simmons, E. H. Linfield, M. Pepper, and D. A. Ritchie, Phys. Rev. B **70**, 245311 (2004).
[49] C. W. J. Beenakker and H. van Houten, Phys. Rev. B **38**, 3232 (1988).
[50] T. J. Thornton, M. L. Roukes, A. Scherer, and B. P. Van de Gaag, Phys. Rev. Lett. **63**, 2128 (1989).
[51] H. Akera and T. Ando, Phys. Rev. B **43**, 11676 (1991).
[52] E. Ditlefsen and J. Lothe, Philos. Mag. **14**, 759 (1966).
[53] B. Reulet, H. Bouchiat, and D. Mailly, Europhys. Lett. **31**, 305

(1995).
[54] B. N. Narozhny, G. Zala, and I. L. Aleiner, Phys. Rev. B **65**, 180202(R) (2002).
[55] It is also possible to obtain a diffusion coefficient from quasi-1D wires which is 1.5 times larger than that from Hall bars. Plotting the data as a function of D from the wires rather than the 2D Hall bars would simply shift all the data by a fixed value. This does not change the D dependence as well as the interpretation of the data at all. Nevertheless, we have chosen to plot all the data as a function of D from the 2D Hall bars because it is difficult to obtain, for example, n_e and l_e only from the wires. In order to define the regime (semiballistic or diffusive), it is necessary to know l_e. Therefore, we have determined D from the Hall bars.
[56] The residual resistance R_{res} defined here is for 20 wires in parallel. The resistance per 1 wire is 20 times larger. When $R_{\mathrm{res}} > 8$ kΩ, the resistance exponentially increases with decreasing temperature, which indicates that the electron system enters the strongly localized regime as detailed in Sec. VII.
[57] H.-P. Wittmann and A. Schmid, J. Low Temp. Phys. **69**, 131 (1987).
[58] D. S. Golubev and A. D. Zaikin, Physica E **40**, 32 (2007), and references therein.
[59] D. S. Golubev and A. D. Zaikin, Phys. Rev. B **59**, 9195 (1999).
[60] D. S. Golubev, A. D. Zaikin, and G. Schön, J. Low Temp. Phys. **126**, 1355 (2002).
[61] In metallic wires, the three-dimensional formula of the GZ theory is applied since all geometric dimensions (L, w, and film thickness t) are larger than l_e.
[62] B. L. Altshuler and A. G. Aronov, in *Electron-Electron Interactions in Disordered Systems*, edited by A. L. Efros and M. Pollak (North-Holland, Amsterdam, 1985).
[63] One could expect a dimensional crossover for the AA correction when the thermal length $L_T = \sqrt{\hbar D / k_B T}$ is larger than w_{eff}. In this case one would expect a deviation from the 1D law at high temperatures. For a diffusion coefficient D of 1000 cm^2/s and an effective width w_{eff} of 1 μm the crossover temperature is on the order of 1 K. Lowering the diffusion coefficient, the crossover temperature should, in principle, move towards lower temperatures. On the other hand, for all diffusion coefficients investigated as well as for all wire widths, we do not observe such a dimensional crossover at temperatures below 1 K. This suggests that the 1D-2D crossover appears only for L_T much smaller than w_{eff}.
[64] I. V. Gornyi and A. D. Mirlin, Phys. Rev. B **69**, 045313 (2004).
[65] D. S. Golubev and A. D. Zaikin, Phys. Rev. B **70**, 165423 (2004).
[66] C. Mora, R. Egger, and A. Altland, Phys. Rev. B **75**, 035310 (2007).
[67] O. Faran and Z. Ovadyahu, Phys. Rev. B **38**, 5457 (1988).
[68] S.-Y. Hsu and J. M. Valles, Phys. Rev. Lett. **74**, 2331 (1995).
[69] F. Tremblay, M. Pepper, R. Newbury, D. A. Ritchie, D. C. Peacock, J. E. F. Frost, G. A. C. Jones, and G. Hill, J. Phys.: Condens. Matter **2**, 7367 (1990).
[70] H. W. Jiang, C. E. Johnson, and K. L. Wang, Phys. Rev. B **46**, 12830 (1992).
[71] F. W. Van Keuls, X. L. Hu, H. W. Jiang, and A. J. Dahm, Phys. Rev. B **56**, 1161 (1997).
[72] S. I. Khondaker, I. S. Shlimak, J. T. Nicholls, M. Pepper, and D. A. Ritchie, Phys. Rev. B **59**, 4580 (1999).
[73] G. M. Minkov, O. E. Rut, A. V. Germanenko, A. A. Sherstobitov, B. N. Zvonkov, E. A. Uskova, and A. A. Birukov, Phys. Rev. B **65**, 235322 (2002).
[74] G. M. Minkov, A. V. Germanenko, and I. V. Gornyi, Phys. Rev. B **70**, 245423 (2004).
[75] G. M. Minkov, A. V. Germanenko, O. E. Rut, A. A. Sherstobitov, and B. N. Zvonkov, Phys. Rev. B **75**, 235316 (2007).
[76] E. Peled, D. Shahar, Y. Chen, E. Diez, D. L. Sivco, and A. Y. Cho, Phys. Rev. Lett. **91**, 236802 (2003).
[77] W. Li, C. L. Vicente, J. S. Xia, W. Pan, D. C. Tsui, L. N. Pfeiffer, and K. W. West, Phys. Rev. Lett. **102**, 216801 (2009).
[78] A. L. Efros and B. I. Shklovskii, J. Phys. C **8**, L49 (1975).
[79] D. Vollhardt and P. Wölfle, Phys. Rev. Lett. **45**, 842 (1980); Phys. Rev. B **22**, 4666 (1980).
[80] N. F. Mott and M. Kaveh, J. Phys. C **14**, L659 (1981).
[81] R. A. Davies and M. Pepper, J. Phys. C **15**, L371 (1982).
[82] A. A. Gogolin and G. T. Zimányi, Solid State Commun. **46**, 469 (1983).
[83] H. L. Zhao *et al.*, Phys. Rev. B **44**, 10760 (1991) and references therein.
[84] It is difficult to distinguish clearly between the variable range hopping model and the self-consistent theory from our results. The same analyses for the conductivity in the strongly localized regime have been performed by Minkov *et al.* (Ref. 73). But they could not identify a reliable mechanism of the conductivity, either.
[85] Note that Eq. (4) is valid only in the weakly localized regime and should not be applicable in the strongly localized regime.
[86] M. E. Gershenson *et al.*, Phys. Rev. Lett. **79**, 725 (1997).
[87] Y. B. Khavin, M. E. Gershenson, and A. L. Bogdanov, Phys. Rev. B **58**, 8009 (1998).
[88] Although L_ϕ for $w_{\mathrm{eff}} = 1130$ nm wide wire is smaller than w_{eff} above $T = 100$ mK, the WL curves can still be fitted well by the 1D WL theory, Eq. (6), over the whole temperature range.
[89] D. J. Thouless, Phys. Rev. Lett. **39**, 1167 (1977).
[90] In Figs. 30(d)–30(f), we have already corrected the electron temperature below 60 mK by using the AA law for another diffusive wire or Hall bar at the same diffusion coefficient D.
[91] Y. B. Khavin, M. E. Gershenson, and A. L. Bogdanov, Phys. Rev. Lett. **81**, 1066 (1998).